



LAWRENCE
LIVERMORE
NATIONAL
LABORATORY

Stellar Astrophysics and a Fundamental Description of Thermonuclear Reactions # 04-ERD-058 Final Report

W.E. Ormand, P. Navratil, S.B. Libby

February 23, 2007

Disclaimer

This document was prepared as an account of work sponsored by an agency of the United States Government. Neither the United States Government nor the University of California nor any of their employees, makes any warranty, express or implied, or assumes any legal liability or responsibility for the accuracy, completeness, or usefulness of any information, apparatus, product, or process disclosed, or represents that its use would not infringe privately owned rights. Reference herein to any specific commercial product, process, or service by trade name, trademark, manufacturer, or otherwise, does not necessarily constitute or imply its endorsement, recommendation, or favoring by the United States Government or the University of California. The views and opinions of authors expressed herein do not necessarily state or reflect those of the United States Government or the University of California, and shall not be used for advertising or product endorsement purposes.

This work was performed under the auspices of the U.S. Department of Energy by University of California, Lawrence Livermore National Laboratory under Contract W-7405-Eng-48.

Stellar Astrophysics and a Fundamental Description of Thermonuclear Reactions – 04-ERD-058

Final report

W. Erich Ormand (PI), L-414, ext: 2-8194, ormand1@llnl.gov
Petr Navrátil (co-PI), L-414, ext: 4-3725, navratil1@llnl.gov
Steve Libby (co-PI), L-473, ext: 2-9785, libby1@llnl.gov

Abstract

Report on the progress achieved in 04-ERD-058. The primary goal of the project was to investigate new methods to provide a comprehensive understanding of how reactions between light nuclei proceed in hot, dense environments, such as stellar interiors. The project sought to develop an entirely new theoretical framework to describe the dynamics of nuclear collisions based on the fundamental nuclear interactions. Based on the new theoretical framework, new computational tools were developed to address specific questions in nuclear structure and reactions. A full study of the true nature of the three-nucleon interaction was undertaken within the formalism of effective field theory. We undertook a preliminary theoretical study of the quantum corrections to electron screening in thermal plasmas to resolve a discrepancy exhibited in previous theoretical approaches

1 Introduction

Understanding the properties of light nuclei is of fundamental interest in physics and crucial to our understanding of stellar evolution and nuclear applications in areas of energy and national security. Light-ion fusion reactions in the pp-chain, which essentially burn protons to form Helium, power the Sun. Just as important, although inconsequential in the generation of energy, are several minority reactions, where uncertainties in the cross section for ${}^3\text{He}(\alpha,\gamma){}^7\text{Be}$ and ${}^7\text{Be}(p,\gamma){}^8\text{B}$ limit our knowledge of neutrino oscillations¹ (from the β -decay of ${}^8\text{B}$ in the Sun). These pp-chain forms the basis a unified picture of the Sun known as the Standard Solar Model (SSM)². Further refinements of the SSM aimed at higher precision constraints on neutrino-oscillation parameters and better understanding of stellar astrophysics will require improved knowledge of fusion reactions in thermal environments. Indeed, Bahcall¹ identifies the reaction ${}^3\text{He}(\alpha,\gamma){}^7\text{Be}$ as the most important reaction limiting the accuracy of the SSM. On the other hand, the $d(t,n){}^4\text{He}$ reaction is central to terrestrially controlled fusion experiments. Naturally, one would think to turn to experiment to obtain these critical cross sections. This, however, turns out to be quite difficult in general because: (1) the astrophysical energies of interest, typically ~ 10 keV, are generally much lower than can be achieved with an accelerator, and the data must be extrapolated to the energy region of interest; (2) at these low-energies, the reaction is severely inhibited by the Coulomb barrier, and the experimental rates are so low as to be background limited; and (3) the target is usually electrically neutral and the screening from the atomic electron cloud substantially affects the cross section, which must then be unfolded. Consequently, theoretical methods would have substantial value in this endeavor. Remarkably, however, prior to our project no fundamental theory for these reactions existed. On top of the nuclear physics issues raised are also questions relating to the effects of electron screening in the thermal plasma, which are quite different than those in the neutral target mentioned above. The primary goal of this LDRD project was to address these last two issues.

Central to developing a fundamental theory for low-energy, light-ion reactions are: (1) understanding the exact nature of the interaction between the constituent protons and neutrons in the nucleus; (2) an accurate theory to describe the structure of a nucleus; and (3) a new theory that incorporates (1) and (2) into a dynamical description of a collision between two nuclei. We address these three issues directly in this project. We developed new computational tools to carry out large-scale nuclear structure calculations for nuclei ranging from the triton to Oxygen. With these tools, we were able to examine the form of the three-nucleon interaction, and place limits on its form and how it affects the structure of nuclei. One of the overarching effects of the three-body interaction is that it is responsible for much of what is often referred to as the “spin-orbit” physics in the nucleus. From this project, we are well on our way to developing a new formalism for describing dynamical processes. Given the obvious complexity of this task, we are accomplishing this in steps. First, we examined clustering effects in nuclei, and using a potential model performed an “ab initio” calculation for the ${}^7\text{Be}(p,\gamma){}^8\text{B}$ reaction. This first generation theory is now being applied to the $d(t,n){}^4\text{He}$ and ${}^6\text{Li}(n,t){}^4\text{He}$ reactions. This effort was followed by a much more fundamental, as well as ambitious, theory obtained by merging our highly successful ab initio, No-core shell model approach with the resonating group method. This will offer a path to a truly ab initio picture of light-ion reactions, and will dramatically improve our overall ability to describe the structure of nuclei, especially unbound resonance states.

Our report is organized in the following manner. In Section 2, we describe the research team, LDRD resources, and leveraged research assets. In Section 3, we outline elements of the project related to nuclear structure, both the development of computational tools and our effort to determine the three-nucleon interaction. In Section 4, the theoretical developments for reaction theory are presented. Results of our studies of the effects of electron screening in plasma environments are described in Section 5. Benefits of this LDRD to LLNL are described in Section 7. The list of publications and invited talks generated from this LDRD are given in Section 6, and concluding remarks are given in Section 8.

2 Research team

This LDRD provided funding for the three years to support approximately 0.6 staff FTE and 0.5 post-doctoral research associate. The primary research staff members were Erich Ormand (N-Division), Petr Navratil (N-Division), and Stephen Libby (V-Division). Over the course of the project, the PI and co-PI secured a small (~\$70K) grant from the DOE Office of Nuclear Physics, which was sufficient to support the remaining half of the post-doctoral researcher. Two post-doctoral researchers worked on this project at 50% effort each. These were: Christen Forssen and Vesselin Gueorguiev. In FY06, Dr. James Vary (Iowa State University) joined our project while on sabbatical leave. Funding was obtained from the University Relations Department at LLNL and this LDRD to support his sabbatical stay at LLNL. His participation provided a substantial benefit to the project, as brought a new set of tools for nuclear structure, with which we were able to fully exploit the high-performance computing environment offered at LLNL. In addition, in FY06, Hai Ah Nam, a graduate student at San Diego State University, applied for and received a graduate student fellowship from a University Relations program at LLNL. She is worked with the PI in FY06 (and will continue to do so until her graduation) on extending the capability of current nuclear structure computer programs. During the last year of the project, funding was requested to support an additional post-doctoral researcher to work on the effects of electron screening in thermal plasmas. Unfortunately, the FY06 budget was reduced to a point below which the additional post-doctoral

researcher could not be supported. Given the overall strength in the team in nuclear theory, the effort towards the electron screening portion of the project was reduced.

3 Nuclear Structure

As mentioned in the introduction, a fundamental theory for light-ion reactions requires two critical ingredients: (1) a full understanding of the interaction between the constituent protons and neutrons, especially the three-nucleon interaction; and (2) a method to accurately describe the structure of the individual nuclei. Naturally, a comprehensive picture of nuclear structure itself requires success in item (1). Towards this end, we have developed a series of computer codes that exploit the power of emerging high-performance computing, especially at LLNL, to perform ab initio calculations for light p-shell nuclei with both two-body and three-body interactions. With these tools in place, we then conducted a systematic study of the properties of the inter-nucleon interactions. In Section 3.1, we outline code development for configuration-interaction methods. In Section 3.2 basic idea behind the ab initio No-core Shell Model is described, and in Section 3.3 we describe the application towards determining the three-nucleon interaction.

3.1 Nuclear Structure Tools

The configuration interaction (CI) methods are among of the most successful methods for providing accurate and detailed descriptions of electronic structure in atoms and nucleonic degrees of freedom in nuclei. Valence particles are spatially confined to a set of orbitals and influence each other via a residual interaction. A mean-field is often used to provide the basis to build a set states, ϕ_i , that we then use to construct the many-body eigenstates of the nuclear Hamiltonian, \hat{H} i.e.,

$$\Phi_\mu = \sum_i c_i \phi_i. \quad (1)$$

Mathematically, the configuration interaction method reduces to a matrix-diagonalization problem by computing the matrix elements, $\mathbf{H}_{ij} = \langle \phi_j | \hat{H} | \phi_i \rangle$ between each of the basis states, and then finding the eigenvalues of the resulting matrix. These eigenvalues then correspond to the physically observable states. Historically, these configuration-interaction methods have been referred to in nuclear physics as the shell model. For a fairly comprehensive review of the application of the shell model in nuclear physics, see refs.^{3,4,5}

The main challenge in configuration interaction methods is to obtain the eigenvalues themselves. This is because the basis dimension can reach 10^7 or more. Of course detailed information on all 10^6 eigenvalues is not needed, as we are particularly interested in the lowest eigenvalues, which we may compare individually with discrete levels measured experimentally. A typical strategy to find the eigenvalues of a matrix is to reduce the matrix to tri-diagonal form. With such large dimensions, methods such as LU-decomposition are numerically inefficient, as it requires we reduce the entire matrix to tri-diagonal form. Instead, we turn the Lanczos method⁶. We start with an arbitrary vector in the Hilbert space, Φ_1 and apply the Hamiltonian to this vector. This leads to a new vector, which we can write as

$$\hat{H}\Phi_1 = \alpha_1\Phi_1 + \beta_1\Phi_2 \quad (2)$$

where the new vector Φ_2 is orthogonal to Φ_1 . We proceed by repeating with applying \hat{H} to Φ_2 giving

$$\hat{H}\Phi_2 = \beta_1\Phi_1 + \alpha_1\Phi_2 + \beta_2\Phi_3.$$

Repeating on Φ_3 , and successive vectors, gives

$$\begin{aligned}
\hat{H}\Phi_1 &= \alpha_1\Phi_1 + \beta_1\Phi_2 \\
\hat{H}\Phi_2 &= \beta_1\Phi_1 + \alpha_2\Phi_2 + \beta_2\Phi_3 \\
\hat{H}\Phi_3 &= \beta_2\Phi_2 + \alpha_3\Phi_3 + \beta_3\Phi_4 \\
\hat{H}\Phi_4 &= \beta_3\Phi_3 + \alpha_4\Phi_4 + \beta_4\Phi_5.
\end{aligned}
\tag{3}$$

Thus, the bringing the matrix into tri-diagonal form is reduced to a series of matrix-vector multiplications and vector dot products to evaluate the quantities α and β . While this is not a very efficient mechanism for bring the whole matrix into tri-diagonal form, it does have one major advantage in that as we increase the number of iterations in the procedure, the eigenvalues of the resultant tri-diagonal matrix converge to extreme eigenvalues of the full matrix. Typically, one finds the lowest ten eigenvalues using approximately 200 iterations regardless of the original dimension. The Lanczos procedure has been the mainstay of configuration-interaction applications to nuclei for several decades now. Prior to our LDRD, efficient codes have been developed that have been applied to nuclear systems with dimensions approaching 10^7 . These codes, however, were limited to two-body interactions and did not exploit parallel computer architectures. Perhaps the most successful of these, which we also utilized during this project for calculations using pure two-body interactions is ANTOINE⁷.

The challenge is to develop an efficient computer program to build up the tri-diagonal matrix of Eq. (3) that also includes the three-nucleon interaction. Two strategies exist to implement the Lanczos method. The first is to pre-compute the Hamiltonian matrix \mathbf{H}_{ij} and store it either on disk or in resident memory. The second, which is the basis of the code ANTOINE, is to compute the action of applying the Hamiltonian to each vector on the fly. We have employed both strategies in this project, as each approach has different advantages and disadvantages that one can exploit depending on the problem at hand. With the addition of the James vary in our collaboration in FY06, we utilized his program MFD, which pre-computes the Hamiltonian matrix and stores it across many processors. For the largest calculations performed in this project, ^{12}C with $N_{\text{max}} = 6$ oscillator quanta (described in the next section), the memory requirements were approximately 2TB and approximately 3500 processors on THUNDER were required. In collaboration with Prof. Calvin Johnson (San Diego State University) in FY02, we began constructing a two-body, on-the-fly computer program, REDSTICK, modeled after the highly successful program ANTOINE, but capable of exploiting parallel computer

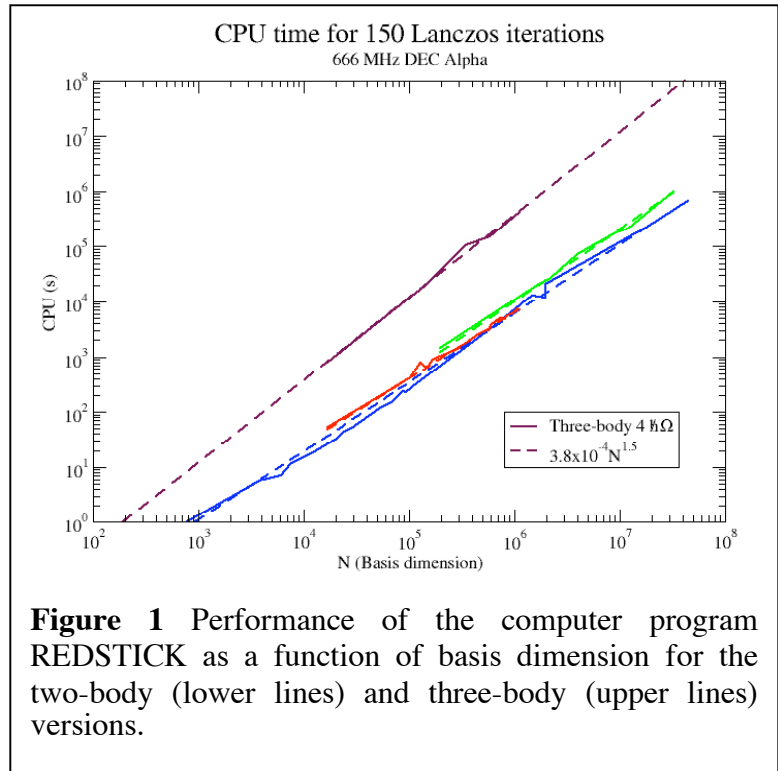


Figure 1 Performance of the computer program REDSTICK as a function of basis dimension for the two-body (lower lines) and three-body (upper lines) versions.

architecture. During this LDRD, we improved the underlying algorithm, and extended it to include three-body interactions. The major difference between MFD and REDSTICK is that since REDSTICK it does not require storing the entire Hamiltonian matrix, it is less memory limited and can execute on an arbitrary number of processors. In cases where the full matrix can be stored in resident memory, MFD is much more efficient, and many of the p-shell applications reported in Section 3.3 were performed with MFD. On the other hand, the memory requirements for $N_{\max} = 8$ calculations are of the order 60TB, which will clearly exceed the capability of most available computers for several years. Consequently, the REDSTICK algorithm offers a promising avenue for progress.

The performance of REDSTICK is shown in Figure 1 for both the two-body and three-body versions as a function of dimension size, N . The two-body program was found to scale as $N^{1.2}$, while the three-body program scales as $N^{1.5}$. The parallel performance for a modest two-body application ($N \sim 10^6$) is shown in Figure 2. The blue line indicates the original parallel algorithm, which shows a saturation at approximately 30 processors. This saturation was largely caused by an improper load balance, where approximately 90% of the work was being done with 10% of the basis. We investigated a different approach, which gives much better scaling out to 150 processors. Overall, scaling with processor number significantly improves with increasing basis dimension.

In the future, the algorithm improvements will be implemented to REDSTICK and the two- and three-body versions will be merged into a common platform. This work will be undertaken with support from a SciDAC-2 grant and with the assistance of Hai Ah Nam, a Ph. D. graduate student (supported with an LLNL graduate student fellowship) in computational science at San Diego State University.

3.2 The No-core Shell Model

A long-standing goal in nuclear structure has been to arrive at a first-principles description of nuclei. Here, at LLNL, we have developed and implemented the highly successful ab initio, No-core Shell Model (NCSM)⁸. The starting point of the NCSM is the nucleon-nucleon (NN) and three-nucleon interaction. Very accurate NN potentials have been developed from NN-scattering data and the ground-state properties of the deuteron. On the other hand, the exact form of the three-nucleon is not yet known, and is the subject of the next section. In order to provide the basis for the many-body calculation, we introduce an oscillator potential in the center-of-mass coordinate (note, the effect of this potential is then later subtracted from the many-body system), which does not affect

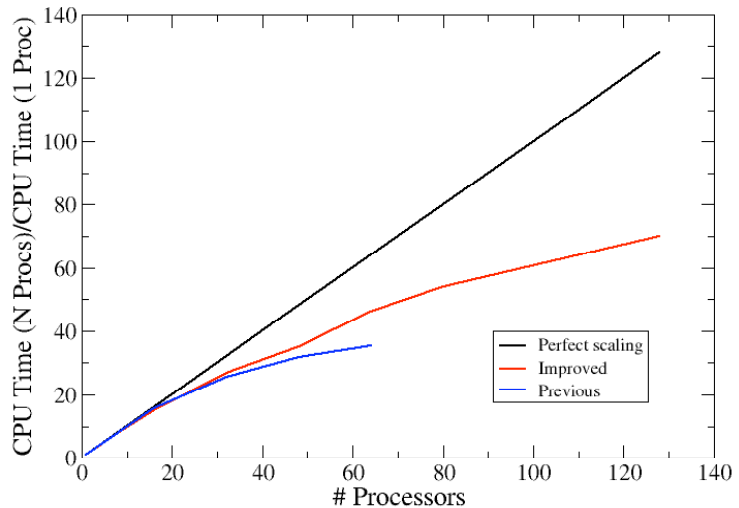


Figure 2 Performance enhancement of the computer program REDSTICK (two-body) as a function of processor number. The blue line indicates a previous inefficient parallel algorithm, while the red line are results from the improved algorithm. The black line represents perfect scaling.

the intrinsic motion and when written in terms of the single-particle coordinates, leads to the many-body harmonic-oscillator Hamiltonian that we then use to construct the many-body Slater determinants. The primary advantages of the oscillator basis are: 1) it provides a basis with a natural truncation scheme that has physical basis in terms of nuclear excitations and 2) when the complete set of basis states with a given number oscillator quanta (defined here as $N_{\max} \hbar\Omega$) is used, it is possible to *exactly* separate the intrinsic and center-of-mass degrees of freedom. An additional parameter is introduced, namely the oscillator parameter, or frequency, $\hbar\Omega$, which sets the physical scale, i.e., the rms radius. Ideally, the dependence on $\hbar\Omega$ diminishes once a large enough basis has been chosen to effectively achieve convergence. With the oscillator basis, we construct the many-body Slater determinants, compute the matrix elements of the Hamiltonian, and, by diagonalizing the resulting matrix, obtain the physical states of the system. For most high-quality NN-potentials this procedure fails because the short-range behavior characteristic of the NN-potential essentially requires an infinite basis.

The infinite basis problem can be remedied with effective interaction theory. The idea is to derive an effective Hamiltonian, H_{eff} , for use within a subset of the full model space, usually denoted as the P -space, so eigenstates of the full Hamiltonian are exactly reproduced. Here, we utilize a unitary transformation based on the method of Lee and Suzuki⁹. An important property of the effective interaction is that it is composed of two-, three-, up to A -body components even if the initial Hamiltonian is only two-body in character. These higher-body components are induced through the projection of the full Hamiltonian onto the P -space. We note that formally, the derivation of H_{eff} is itself as difficult as solving the full problem. Instead, we approach H_{eff} by utilizing a cluster approximation, with the knowledge that we are guaranteed convergence to the exact effective interaction as we continually extend the size of the P -space and/or increase the number of cluster nucleons in H_{eff} . From the practical standpoint, the computational complexity increases dramatically when one increases either the size of the basis or the number of cluster nucleons, a , in H_{eff}^a . Since we will now address the effects of the three-nucleon interaction on nuclear structure, we presently truncate the effective interaction to $a = 3$.

3.3 *The three-nucleon interaction*

In this section, we outline our application of our new CI tools to studying the form of the inter-nucleon interactions and the structure of nuclei ranging from the triton to Oxygen. Our starting point is the interaction between nucleons, which, of course, is determined by the strong interaction as governed by the quantum chromodynamics (QCD). Although in principle, nuclear interactions could be obtained from lattice QCD calculations, this is not feasible due to extreme computational limitations. Instead, previous works relied on either purely empirical potential models, such as the AvN (Argonne potentials)¹⁰, or those based on meson-exchange, such as the Bonn potentials¹¹, which were fit to nucleon-nucleon phase shifts. It is worth noting that even in this case of the Bonn potential, a new empirical, and unphysical, meson was required to obtain a proper description of the nucleon-nucleon phase shifts. This empirical situation is made even more unsatisfying when we include three-nucleon potentials, which are required for a proper description of nuclear binding and structure. Our past studies utilized the Tucson-Melbourne interaction¹², which is guided by two-pion exchange and the exchange of intermediate Δ particles, while the ab initio Green's Function Monte Carlo work (at Argonne and LANL) used a purely empirical form for the three-nucleon interaction¹³. Until very recently, there has been no overall consistent framework to derive the various components of the inter-nucleon interactions. A cure for this inconsistency was introduced by Weinberg¹⁴ in what has been come to be known as effective field theory (EFT). EFT is based on QCD through chiral perturbation theory and provides an elegant framework for mapping out the

leading degrees of freedom in the nuclear Hamiltonian. Chiral symmetry imposes constraints on the possible momentum and spin dependencies in the nuclear forces. In addition, a momentum cutoff is introduced leading to a natural power counting scheme that limits the number of interaction terms in the nuclear Hamiltonian. With EFT, one derives the nuclear forces up to a given order, manifestly including all the relevant QCD degrees of freedom to that order. EFT potentials are often defined by the order in the expansion, e.g., leading order, next-to-leading order (NLO), next-to-next-to-leading order (N²LO), etc.

It is important to note that EFT potentials are not completely devoid of empiricism either, but rather give a framework for expanding and quantifying the nuclear Hamiltonian. The framework of EFT is shown schematically in Figure 3 up to N³LO. Note that with EFT, a three-nucleon interaction enters at N²LO, while even a four-body term enters at N³LO. As an expansion for the nuclear force, a set of parameters define the strength of each diagram and the various components as given by chiral

perturbation theory. For the nucleon-nucleon interaction, these parameters have been determined up to N³LO by fitting to nucleon-nucleon phase shifts for incident energies up to 300 MeV¹⁵. While at this stage there are 24 parameters in the nucleon-nucleon sector, there are only two additional parameters for the three-nucleon interaction; the strength of the remaining diagram (e.g., two-pion exchange) is completely determined by the nucleon-nucleon coupling constants. The diagrams for these two parameters are circled in Figure 3 and denoted by C_D and C_E . We note that while additional pion-exchange diagrams are introduced at N³LO, no additional parameters are introduced. Again, the strengths of the other diagrams are completely determined by coupling constants in the nucleon-nucleon sector. Ideally, as in the

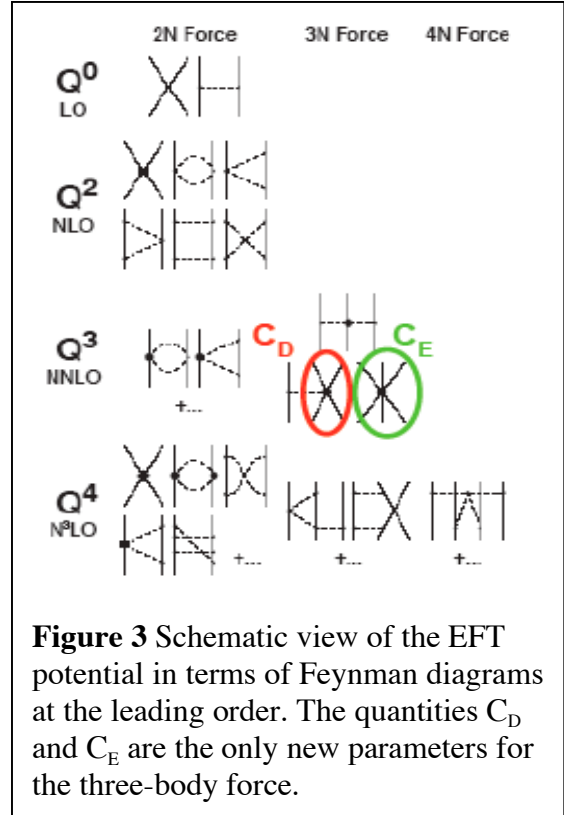


Figure 3 Schematic view of the EFT potential in terms of Feynman diagrams at the leading order. The quantities C_D and C_E are the only new parameters for the three-body force.

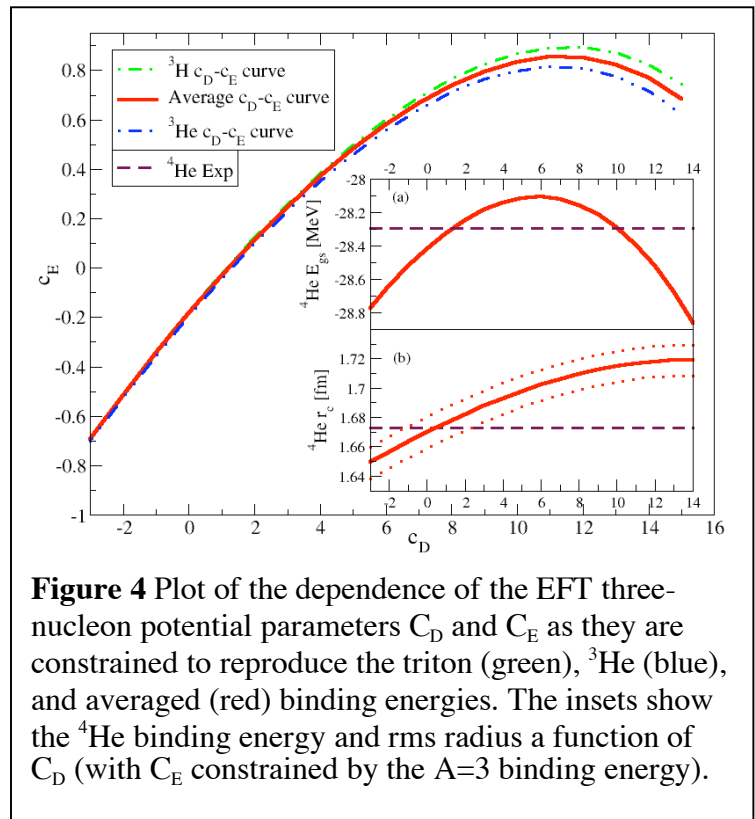


Figure 4 Plot of the dependence of the EFT three-nucleon potential parameters C_D and C_E as they are constrained to reproduce the triton (green), ^3He (blue), and averaged (red) binding energies. The insets show the ^4He binding energy and rms radius a function of C_D (with C_E constrained by the $A=3$ binding energy).

nucleon-nucleon sector, C_D and C_E would be fit to a wide range of three-nucleon scattering data, from say p+d or n+d scattering, but at present there is insufficient data. Alternatively, we turn to bound-state three- and higher-body systems; namely, ^3H , ^3He , and ^4He and p-shell nuclei.

In this LDRD, we performed an extensive study of the three-nucleon potential to determine the C_D and C_E constants at the level of $N^2\text{LO}$. This work made extensive use of LLNL computing facilities (over 800,000 CPU hrs on THUNDER), and was submitted¹⁶ as an article to Physical Review Letters in January 2007. The NCSM is uniquely positioned to perform this study as it is the only method available today capable of performing calculations with EFT potentials for nuclei heavier than ^4He . Figure 4 shows a parabola in C_D and C_E where the binding energies of ^3H (green), ^3He (blue) are exactly reproduced. We note the slight difference in the red and green curves, with the average value denoted by the solid red line. This difference is largely due to a slight increase in the rms radius. In the insets, we show the binding energy of ^4He (top inset) and rms radius (bottom inset) as a function of C_D (the value of C_E was fixed to reproduce the average $A=3$ binding energy). From the figure, we see that the $A=3$ system by itself is insufficient to constrain the three-body EFT parameters. Indeed, at $N^2\text{LO}$, even the ^4He binding energy is only slightly sensitive to the parameters, but the exhibited spread of 200 keV is also insufficient to constrain the EFT parameters, as this we can expect some dependence from the additional $N^3\text{LO}$ terms; in particular the four-body term is expected to contribute approximately 200 keV to the ^4He binding energy. On the other hand, a stronger dependence on C_D is shown by the rms radius, where a stronger disagreement with experiment is shown for $C_D > 3$.

We have also performed large-basis calculations for p-shell nuclei to examine the effects the three-nucleon interaction on nuclear structure, and the sensitivity to the C_D and C_E parameters. In Figure 5 are the results of calculations for ^6Li , ^{10}B , and ^{12}C for different model spaces ($N_{\text{max}} \hbar\Omega$) in comparison with experimental data. In the upper panel the static quadrupole moment for ^6Li is

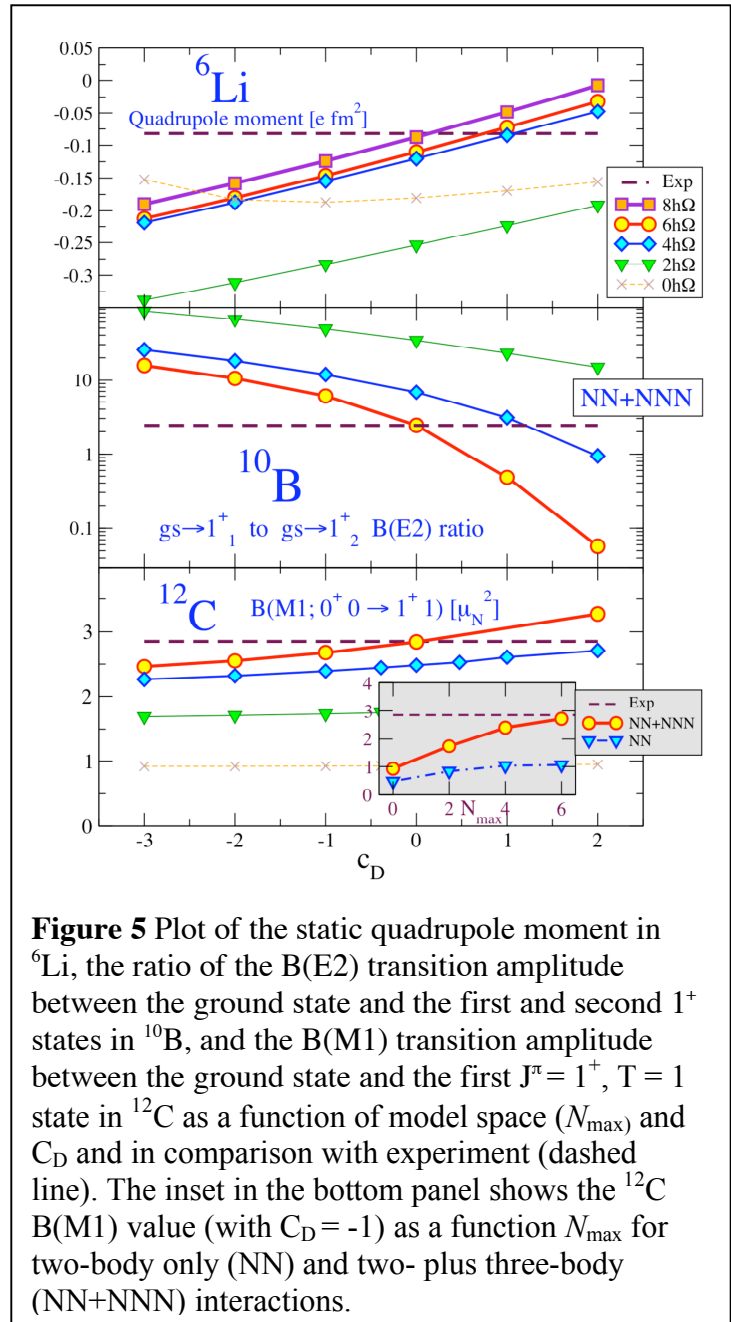
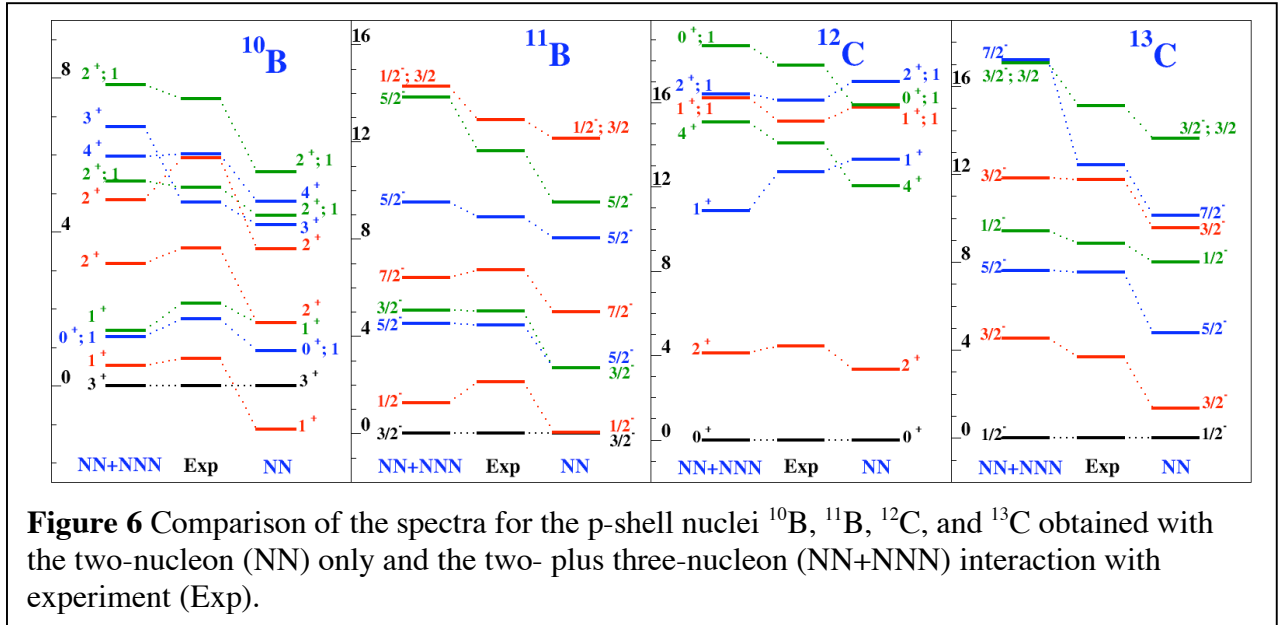


Figure 5 Plot of the static quadrupole moment in ^6Li , the ratio of the $B(E2)$ transition amplitude between the ground state and the first and second 1^+ states in ^{10}B , and the $B(M1)$ transition amplitude between the ground state and the first $J^\pi = 1^+$, $T = 1$ state in ^{12}C as a function of model space (N_{max}) and C_D and in comparison with experiment (dashed line). The inset in the bottom panel shows the ^{12}C $B(M1)$ value (with $C_D = -1$) as a function N_{max} for two-body only (NN) and two- plus three-body (NN+NNN) interactions.

plotted. In the middle panel, the ratio of the B(E2) transition amplitude between the ground state and the first and second 1^+ states in ^{10}B is shown. Finally, in the bottom panel is B(M1) transition amplitude in ^{12}C between the ground state and the first $J^\pi = 1^+$, $T = 1$ state. For each observable, better agreement with experiment is achieved for $-1 \leq C_D \leq 1$. The small insert in the bottom panel also shows a comparison of this same B(M1) value calculated with $C_D = -1$ with experiment as a function of model space (N_{max}) with two-body only (NN) and two- plus three-body (NN+NNN) interactions. Overall, one finds that the NN-interaction by itself significantly underestimates the B(M1) value, and that good agreement with experiment is achieved with the NN+NNN interaction. This is an important result, as it indicates that the three-nucleon interaction has a strong effect on spin observables, and is likely responsible for the observed strengths in Gamow-Teller β -decay.



In addition to the transition amplitudes shown in Figure 5, the NNN interaction also affects the low-lying spectrum. We illustrate this with Figure 6, where the spectra for ^{10}B , ^{11}B , ^{12}C , and ^{13}C (with $C_D = -1$) are shown for NN and NN+NNN interactions in comparison with experiment. In each case, significantly better agreement with experiment is achieved with the three-nucleon interaction. The result of our work was that at the present level with the inclusion of three-body diagrams at $N^2\text{LO}$ the values $C_D = -1$ and $C_E = -0.346$ represent the best overall choice. Further, it is abundantly clear that the three-nucleon interaction significantly affects the structure of nuclei and is largely responsible for what we refer to as the spin-orbit properties of nuclei. Failure to include the affects of the NNN interaction will lead to a substantial degradation in our ability to predict nuclear properties. The main challenge for nuclear structure physicists in the future is to integrate the effects of the NNN interaction into their models.

Our future plans for the NCSM, which will be supported through a SciDAC-2 grant as well as a DOE/SC/NP grant will be to extend the description of the three-nucleon interaction to include all the $N^3\text{LO}$ diagrams, to extend the calculations for light p-shell nuclei to $N_{\text{max}}=8$, and to understand the effects of the weak four-body interaction that is apparent at $N^3\text{LO}$.

4 Nuclear Reactions

Low-energy nuclear reactions are important for the physics of stellar evolution and potential energy sources. Light-ion fusion reactions in the pp-chain power the Sun, and uncertainty in the minority reactions ${}^7\text{Be}(p, \gamma){}^8\text{B}$ and ${}^3\text{He}(\alpha, \gamma){}^7\text{Be}$ limits our knowledge of neutrinos. The helium burning in massive stars converts ${}^4\text{He}$ in ${}^{12}\text{C}$ and ${}^{16}\text{O}$. There are still unanswered questions concerning the sequential fusion of three ${}^4\text{He}$ to form ${}^{12}\text{C}$ and the ${}^{12}\text{C}(\alpha, \gamma){}^{16}\text{O}$ reaction that determines the C/O ratio and future evolution of stars. On the other hand, the $d(t, n){}^4\text{He}$ reaction is central to terrestrially controlled fusion experiments. These reactions in the low-energy regime relevant for astrophysics processes are hard, or even impossible, to measure experimentally. Thus, a predictive theoretical description of these reactions is imperative. Such a description can only be built upon a truly consistent and *ab initio* description of the structure of light nuclei. It was the goal of our project to develop an *ab initio* approach to low-energy light-ion reactions. The foundation for this approach was the *ab initio* no-core shell model (NCSM), a method capable to describe nuclear structure of light nuclei starting from modern inter-nucleon interactions.

It is a challenging task to extend the *ab initio* methods to describe nuclear reactions. Our ultimate goal to solve this challenge is to couple the NCSM with the resonating group method (RGM), a microscopic technique in which the many-body problem is mapped onto various channels of nucleon clusters and their relative motion. There are several steps that needs to be taken to achieve this goal. One of them is the understanding the cluster structure of the NCSM eigenstates, i.e. the calculation of the channel cluster-form factors (or cluster overlap integral or reduced width amplitude for two-body decay). Those can then, e.g., be integrated to obtain the spectroscopic factors. It should be noted that the channel cluster form factors and the spectroscopic factors are important not just to the low-energy nuclear reactions but also for the understanding of direct reactions. The spectroscopic factors are extracted from experimental measurements.

The principal foundation of the *ab initio* NCSM approach is the use of effective interactions appropriate for the large but finite basis spaces employed in the calculations. These effective interactions are derived from the underlying realistic inter-nucleon potentials through a unitary transformation in a way that guarantees convergence to the exact solution as the basis size increases. For the basis, one uses antisymmetrized A -nucleon harmonic-oscillator (HO) states that span the complete $N_{\text{max}} \hbar\Omega$ space. A disadvantage of the HO basis is its unphysical asymptotic behavior, a problem that must be dealt with by using a large basis expansion and/or a renormalization. On the other hand, the nuclear system is translationally invariant and, in particular in the case of light nuclei, it is important to preserve this symmetry. The HO basis is the only basis that allows a switch from Jacobi coordinates to single particle Cartesian coordinates without violating the translational invariance. Consequently, one may choose the coordinates according to whatever is more efficient for the problem at hand. In practice, it turns out that the $A=3$ and $A=4$ system is the easiest solved in the Jacobi basis. For systems with $A>4$, it is by far more advantageous to use the Cartesian coordinates and the Slater determinant (SD) basis and employ the powerful shell model codes that rely on the second quantization techniques. While the NCSM eigenenergies are independent on the choice of coordinates, the eigenfunctions obtained in the Cartesian coordinate SD basis include a $0\hbar\Omega$ spurious center of mass (CM) component.

Our goal was to calculate the channel cluster form factors as well as any other quantities needed for the development of the reactions theory regardless of the choice of coordinates. Obviously, the most desired case is the one corresponding to the most efficient choice, i.e., the projectile, that is the lighter nucleus of the binary system, consisting of $a\leq 4$ nucleons described by a Jacobi coordinate wave function, while the A -nucleon composite system and the $A-a$ nucleon target,

that is the heavier nucleus of the binary system, described by wave functions expanded in the SD basis. To obtain the physical, translationally invariant cluster form factors we must remove completely the spurious CM components.

We solved the task of calculating the channel cluster form factors and spectroscopic factors in the first year of the project. The details were published in Ref. ¹⁷. Here, we briefly illustrate the channel cluster form factor calculation. Let's consider a composite system of A nucleons, a projectile of a nucleons and a target of $A-a$ nucleons. All the nuclei are described by eigenstates of the NCSM effective Hamiltonians expanded in the HO basis with identical HO frequency and the same (for the eigenstates of the same parity) or differing by one unit of the HO excitation (for the eigenstates of opposite parity) definitions of the model space. We limit ourselves to $a \leq 4$ projectiles that can be efficiently described by a Jacobi-coordinate HO wave functions. The target and the composite system is assumed to be described by Slater determinant single-particle HO basis wave functions which is more efficient for $A > 4$. Let us introduce a projectile-target wave function

$$\begin{aligned} & \langle \vec{\xi}_1 \dots \vec{\xi}_{A-a-1} \eta'_{A-a} \hat{\eta}_{A-a} \vec{\vartheta}_{A-a+1} \dots \vec{\vartheta}_{A-1} | \Phi_{\alpha I_1, \beta I_2; s l}^{(A-a, a) J M}; \delta_{\eta_{A-a}} \rangle \\ &= \sum (I_1 M_1 I_2 M_2 | s m_s) (s m_s l m_l | J M) \frac{\delta(\eta_{A-a} - \eta'_{A-a})}{\eta_{A-a} \eta'_{A-a}} Y_{l m_l}(\hat{\eta}_{A-a}) \\ & \times \langle \vec{\xi}_1 \dots \vec{\xi}_{A-a-1} | A - a \alpha I_1 M_1 \rangle \langle \vec{\vartheta}_{A-a+1} \dots \vec{\vartheta}_{A-1} | a \beta I_2 M_2 \rangle, \end{aligned}$$

The calculation of the cluster form factor

$$\begin{aligned} g_{A-a \alpha I_1, a \beta I_2; s l}^{A \lambda J T}(\eta_{A-a}) &= \langle A \lambda J | \mathcal{A} \Phi_{\alpha I_1, \beta I_2; s l}^{(A-a, a) J}; \delta_{\eta_{A-a}} \rangle \\ &= \sqrt{\frac{A!}{(A-a)! a!}} \sum_n R_{n l}(\eta_{A-a}) \langle A \lambda J | \Phi_{\alpha I_1, \beta I_2; s l}^{(A-a, a) J}; n l \rangle, \end{aligned}$$

can then be done in two steps. First, using the relation between the SD and Jacobi coordinate eigenstates

$$\langle \vec{r}_1 \dots \vec{r}_A | A \lambda J M \rangle_{SD} = \langle \vec{\xi}_1 \dots \vec{\xi}_{A-1} | A \lambda J M \rangle \varphi_{000}(\sqrt{A} \vec{R}),$$

for both the composite and the target eigenstate and the HO wave function transformations, we obtain

$${}_{SD} \langle A \lambda J | \mathcal{A} \Phi_{\alpha I_1, \beta I_2; s l}^{(A-a, a) J}; n l \rangle_{SD} = \langle n l 0 0 l | 0 0 n l \rangle_{\frac{a}{A-a}} \langle A \lambda J | \mathcal{A} \Phi_{\alpha I_1, \beta I_2; s l}^{(A-a, a) J}; n l \rangle,$$

with a general HO bracket due to the CM motion. The $n l$ in the above equations refers to a replacement of $\delta_{\eta_{A-a}}$ by the HO $R_{n l}(\eta_{A-a})$ radial wave function. Second, we relate the SD overlap to a linear combination of matrix elements of a creation operators between the target and the composite eigenstates

$${}_{SD} \langle A \lambda J | a_{m_1 h_1}^+ \dots a_{n_a a_a}^+ | A - a \alpha I_1 \rangle_{SD}$$

Such matrix elements are easily calculated by shell-model codes. To obtain the channel cluster form factor we use the second equality in the equation for $g(\eta_{A-a})$. The spectroscopic factor is obtained by integrating the square of the channel cluster form factor.

As an example, we present the results for the ${}^7\text{Li} \leftrightarrow {}^4\text{He} + t$ channel cluster form factors in Figure 7. Apart from the large overlap integrals and spectroscopic factors for the bound $3/2^-_1$ and $1/2^-_1$ states, we find these quantities to be large also for the first excited $7/2^-_1$ and the first excited $5/2^-_1$ state. Both these states appear as resonances in the ${}^4\text{He} + t$ cross section. The other system involving ${}^7\text{Li}$ as the composite nucleus that we investigated is ${}^6\text{Li} + n$. As in the ${}^7\text{Li} \leftrightarrow {}^4\text{He} + t$ case, we observe large overlap integrals and spectroscopic factors for the two bound states $3/2^-_1$ and $1/2^-_1$. Contrary to the ${}^7\text{Li} \leftrightarrow {}^4\text{He} + t$ case, however, we find a large overlap integral and spectroscopic factor for the $5/2^-_2$

state. The lowest $7/2^-_1$ and $5/2^-_1$ states have negligible overlap integrals for the ${}^6\text{Li}+n$ system. The large overlap integral and the spectroscopic factor for the $5/2^-_2$ state is consistent with the observed resonance in the ${}^6\text{Li}+n$ cross section.

Another important nuclear structure input into nuclear reaction calculations are the one-body densities. These quantities are relevant not just for the low-energy nuclear reactions, the main focus of our project, but also for the direct reactions that involve projectiles of intermediate

energies. The one-body nuclear densities serve as an input to folding approaches to constructing the optical potentials. To fully utilize the *ab initio* NCSM nuclear structure for this purpose, the spurious center-of-mass contribution must be removed from the calculated density obtained in the SD basis. We developed a new procedure of calculating the translationally invariant density. The details were published in Ref.¹⁸. Here we briefly outline the result. The nuclear density operator is defined as

$$\rho_{op}(\vec{r}) = \sum_{i=1}^A \delta(\vec{r} - \vec{r}_i) = \sum_{i=1}^A \frac{\delta(r - r_i)}{r r_i} \sum_m Y_{lm}(\hat{r}_i) Y_{lm}^*(\hat{r}) .$$

The physical density should depend on the coordinate measured from the CM of the nucleus, $\vec{r} - \vec{R}$. Using the transformation properties of the HO wave functions, it is possible to relate the physical density to the standard one-body density matrix elements computed in shell model codes from eigenstates obtained in the Slater determinant basis. The final expression is

$$\begin{aligned} & \langle A\lambda_f J_f M_f | \rho_{op}(\vec{r} - \vec{R}) | A\lambda_i J_i M_i \rangle = \left(\frac{A}{A-1}\right)^{3/2} \frac{1}{J_f} \sum (J_i M_i K k | J_f M_f) Y_{Kk}^*(\vec{r} - \vec{R}) \\ & \times R_{nl} \left(\sqrt{\frac{A}{A-1}} |\vec{r} - \vec{R}\rangle\right) R_{n'l'} \left(\sqrt{\frac{A}{A-1}} |\vec{r} - \vec{R}\rangle\right) (-1)^K \frac{\hat{l}'}{\hat{l}_1 \hat{l}_2} (10l'0 | K0) (M^K)^{-1}_{nl'n'l', n_1 l_1 n_2 l_2} \\ & \times \langle l_1 \frac{1}{2} j_1 || Y_K || l_2 \frac{1}{2} j_2 \rangle \frac{1}{\hat{K}} \text{SD} \langle A\lambda_f J_f || (a_{n_1 l_1 j_1}^\dagger \bar{a}_{n_2 l_2 j_2})^{(K)} || A\lambda_i J_i \rangle_{\text{SD}} , \end{aligned}$$

where the sum is restricted to both $l+l'+K$ and l_1+l_2+K even. The λ_i and λ_f are the additional quantum numbers that classify the initial and final state, respectively. The matrix M^K is defined as

$$\begin{aligned} (M^K)_{n_1 l_1 n_2 l_2, n l n' l'} &= \sum_{N_1 L_1} (-1)^{l+l'+K+L_1} \left\{ \begin{array}{ccc} l_1 & L_1 & l \\ l' & K & l_2 \end{array} \right\} \hat{l}' \\ &\times \langle nl00l | N_1 L_1 n_1 l_1 l \rangle \frac{1}{A-1} \langle n'l'00l' | N_1 L_1 n_2 l_2 l' \rangle \frac{1}{A-1} . \end{aligned}$$

As an illustration of the significance of the spurious CM removal, we calculated the ${}^6\text{He}$ physical density obtained using the above equation and the shell-model density from

$$\text{SD} \langle A\lambda_f J_f M_f | \rho_{op}(\vec{r}) | A\lambda_i J_i M_i \rangle_{\text{SD}}$$

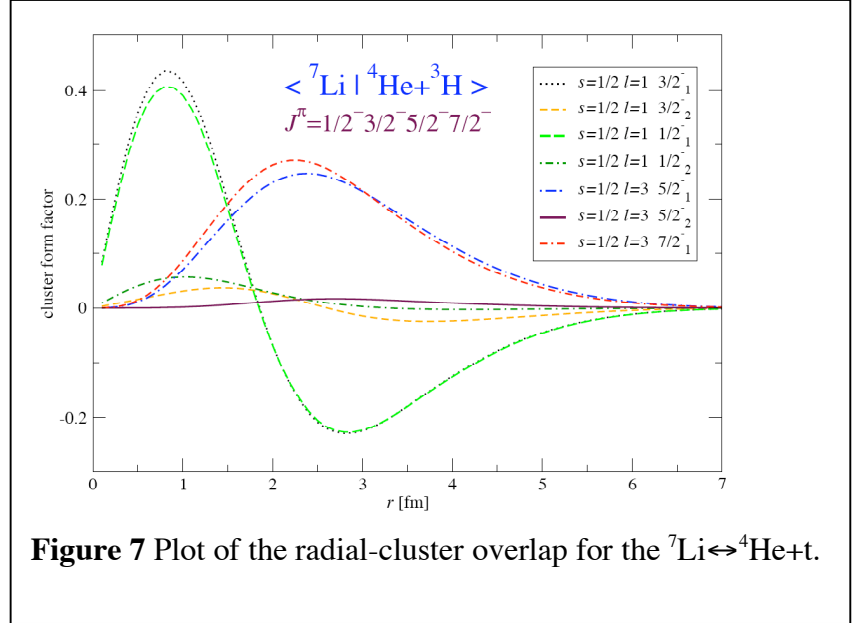


Figure 7 Plot of the radial-cluster overlap for the ${}^7\text{Li} \leftrightarrow {}^4\text{He} + t$.

In Figure 9, the proton and the neutron monopole ground state densities are shown. The full lines correspond to the physical densities calculated according to the above equations while the dashed lines correspond to the shell-model densities that contain the spurious center-of-mass contribution. A particularly significant impact of the exact removal of the spurious center-of-mass motion is found for the spin-orbit part of the optical potential proportional to the derivative of the nuclear density.

We developed a capability to perform direct reaction coupled channel calculations with the optical potentials obtained by folding from our *ab initio* NCSM translationally invariant densities. As an example of a calculation of this type, in Figure 8 we show our elastic cross section calculation for the $p+{}^6\text{Li}$ and ${}^6\text{He}+p$ reactions at intermediate energies.

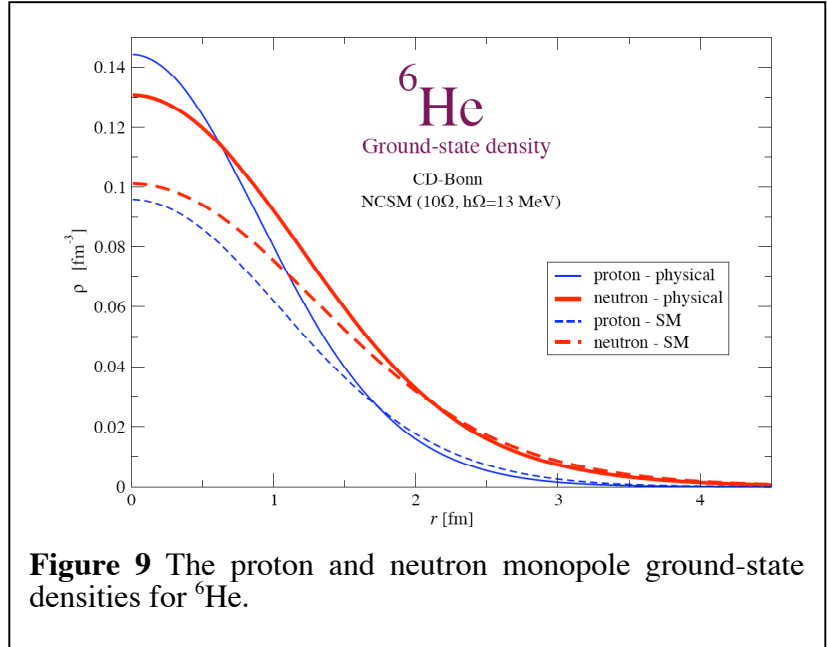


Figure 9 The proton and neutron monopole ground-state densities for ${}^6\text{He}$.

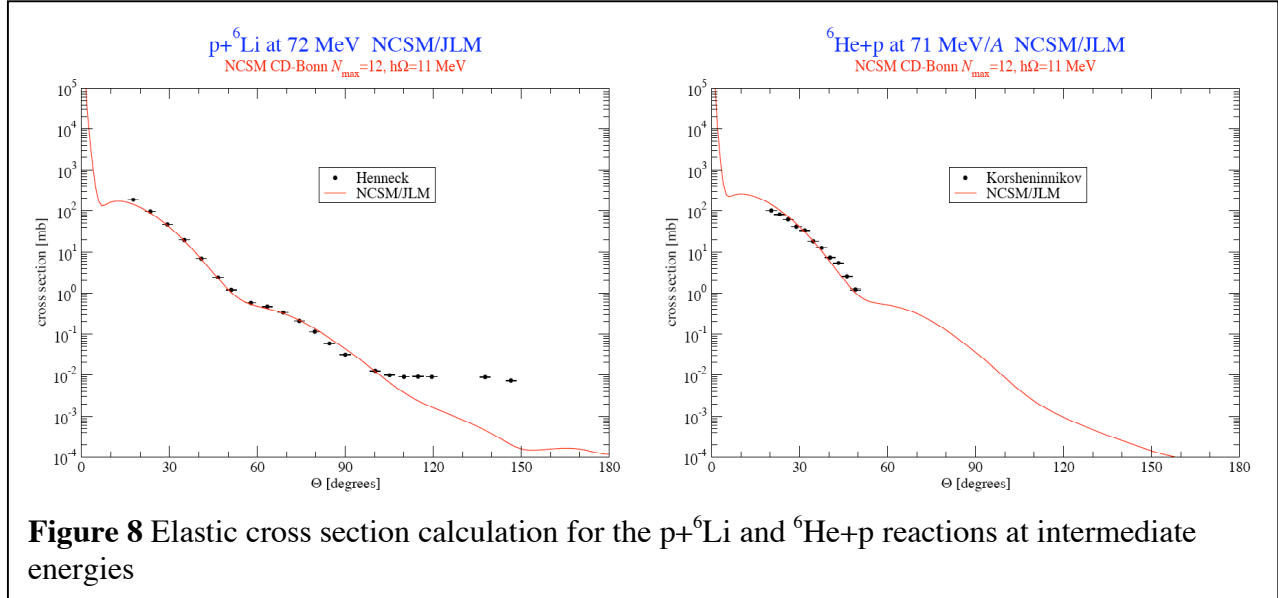


Figure 8 Elastic cross section calculation for the $p+{}^6\text{Li}$ and ${}^6\text{He}+p$ reactions at intermediate energies

Once we achieved the capability to calculate the channel cluster form factors from our *ab initio* NCSM wave functions, a possibility opened up for us to immediately investigate the S-factors (cross sections) of reactions important for astrophysics; even before developing the full *ab initio* reaction theory. The S-factors of radiative capture reactions at low energies, i.e. energies relevant for astrophysics processes, depend strongly on the description of the bound states but only very weakly on the scattering states. Therefore, it is quite sensible to combine our *ab initio* channel cluster form factors obtained for the bound states with potential model description of scattering

states involved in the investigated capture reaction. The only issue we have to deal with is the correction of the asymptotic tail of the cluster form factors that is not correct in our NCSM calculations that rely on the HO basis expansion. Since the asymptotic behavior is known, it is straightforward to perform the corrections.

Towards this end, we investigated the ${}^7\text{Be}(p,\gamma){}^8\text{B}$, ${}^3\text{He}(\alpha,\gamma){}^7\text{Be}$, ${}^3\text{H}(\alpha,\gamma){}^7\text{Li}$ and ${}^{10}\text{Be}(n,\gamma){}^{11}\text{Be}$ capture reactions. The ${}^7\text{Be}(p,\gamma){}^8\text{B}$ capture reaction serves as an important input for understanding the solar neutrino flux. Recent experiments have determined the neutrino flux emitted from ${}^8\text{B}$ with a precision of $\sim 9\%$. On the other hand, theoretical predictions have uncertainties of the order of 20%. The theoretical neutrino flux depends on the ${}^7\text{Be}(p,\gamma){}^8\text{B}$ S-factor. Many experimental and theoretical investigations studied this reaction. Experiments were performed using direct techniques with proton beams and ${}^7\text{Be}$ targets as well as by indirect methods when a ${}^8\text{B}$ beam breaks up into ${}^7\text{Be}$ and proton. Theoretical calculations needed to extrapolate the measured S-factor to the astrophysically relevant Gamow energy were performed with several methods: the R-matrix parametrization, the potential model, and the microscopic cluster models.

In our work, we discuss the first calculation of the ${}^7\text{Be}(p,\gamma){}^8\text{B}$ S-factor starting from *ab initio* wave functions of ${}^8\text{B}$ and ${}^7\text{Be}$. It should be noted that the aim of *ab initio* approaches is to predict correctly absolute cross sections (S-factors), not only relative cross sections. The full details of our ${}^7\text{Be}(p,\gamma){}^8\text{B}$ investigation were published in Refs. ^{19,20}.

From the ground state wave functions of ${}^7\text{Be}$ and ${}^8\text{B}$ obtained in the large-scale *ab initio* NCSM calculations, we calculated the channel cluster form factors. The two most important channels are the *p*-waves, $l=1$, with the proton in the $j=3/2$ and $j=1/2$ states, $\vec{j} = \vec{l} + \vec{s}$, $s=1/2$. In these channels, we obtain the spectroscopic factors of 0.96 and 0.10, respectively. The dominant $j=3/2$ (the less important $j=1/2$) overlap integral is presented in the left (right) panel of Fig. 4 by the full line. The CD-Bonn 2000 NN potential, the $10\hbar\Omega$ model space and the HO frequency of $\hbar\Omega=12$ MeV were used. Despite the fact, that a very large basis was employed in the present calculation, it is apparent that the overlap function is nearly zero at about 10 fm. This is a consequence of the HO basis asymptotics. The proton capture on ${}^7\text{Be}$ to the weakly bound ground state of ${}^8\text{B}$ associated dominantly by the *E1* radiation is a peripheral process. Consequently, the overlap integral with an incorrect asymptotic behavior cannot be used to calculate the S-factor.

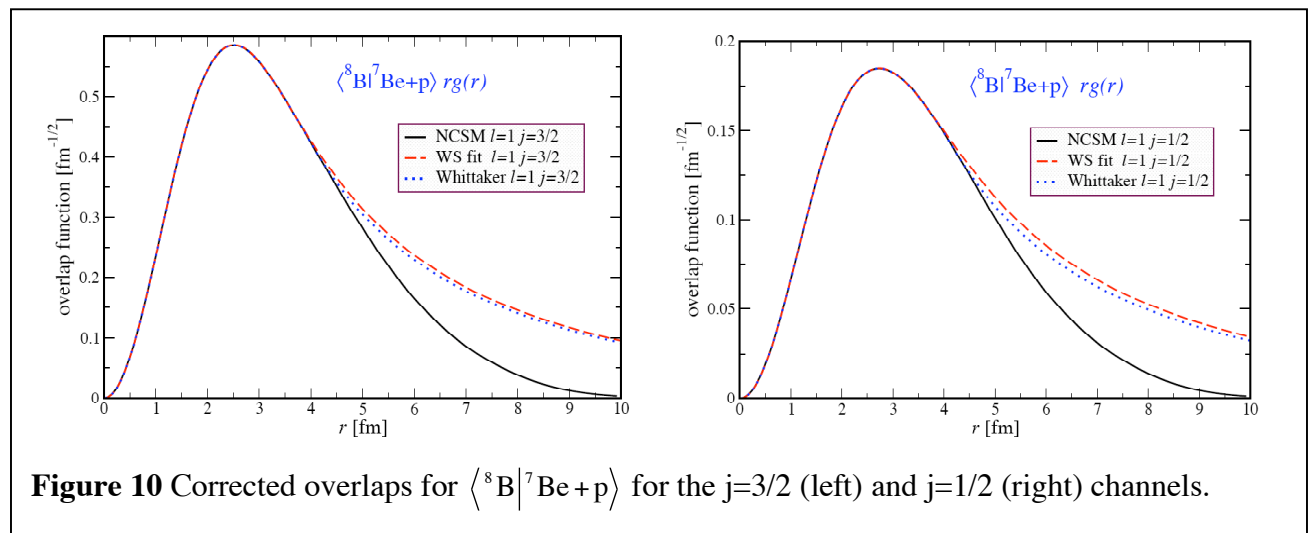


Figure 10 Corrected overlaps for $\langle {}^8\text{B} | {}^7\text{Be} + p \rangle$ for the $j=3/2$ (left) and $j=1/2$ (right) channels.

We expect, however, that the interior part of the overlap function is realistic. It is then straightforward to correct its asymptotics. One possibility we explored utilizes solutions of a

Woods-Saxon (WS) potential. In particular, we performed a least-square fit of a WS potential solution to the interior of the NCSM overlap in the range of 0-4 fm. The WS potential parameters were varied in the fit under the constraint that the experimental separation energy of ${}^7\text{Be}+p$, $E_0=0.137$ MeV, was reproduced. In this way we obtain a perfect fit to the interior of the overlap integral and a correct asymptotic behavior at the same time. The result is shown in Figure 10 by the dashed line. Another possibility is a direct matching of logarithmic derivatives of the NCSM overlap integral and the Whittaker function. The corrected overlap using the Whittaker function matching is shown in Figure 10 by a dotted line. In general, we observe that the approach using the WS fit leads to deviations from the original NCSM overlap starting at a smaller radius. In addition, the WS solution fit introduces an intermediate range from about 4 fm to about 6 fm, where the corrected overlap deviates from both the original NCSM overlap and the Whittaker function. Perhaps, this is a more realistic approach compared to the direct Whittaker function matching. In any case, by considering the two alternative procedures we are in a better position to estimate uncertainties in our S-factor results. The range used in the least-square fit is not arbitrary but varies from channel to channel. The aim is to use as large range as possible, while at the same time preserve the NCSM overlap integral as accurately as possible in that range. Concerning the discussed example (dashed lines in Fig. 4), we note that extending the range beyond 4 fm leads to a worse fit. Finally, we note that the alternative procedure of the direct Whittaker function matching is completely unique.

The S-factor for the reaction ${}^7\text{Be}(p,\gamma){}^8\text{B}$ also depends on the continuum scattering wave function. Since the largest part of the integrand stays outside the nuclear interior, one expects that the continuum wave functions are well described by a potential model. We chose a WS potential that was fitted to reproduce the p -wave 1^+ resonance in ${}^8\text{B}$. It was argued that such a potential is also suitable for the description of s - and d -waves.

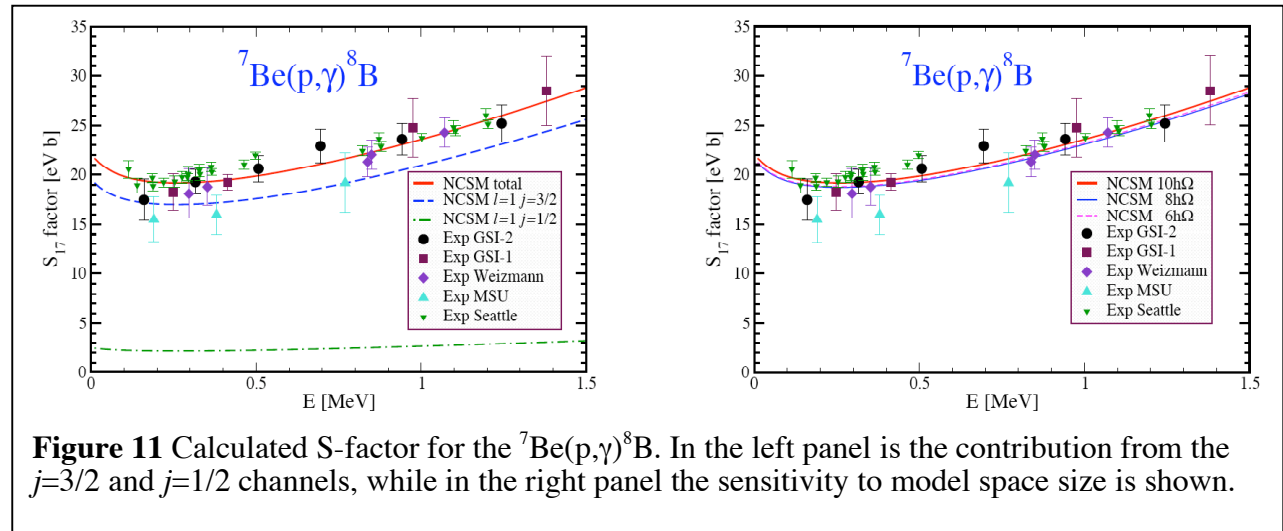
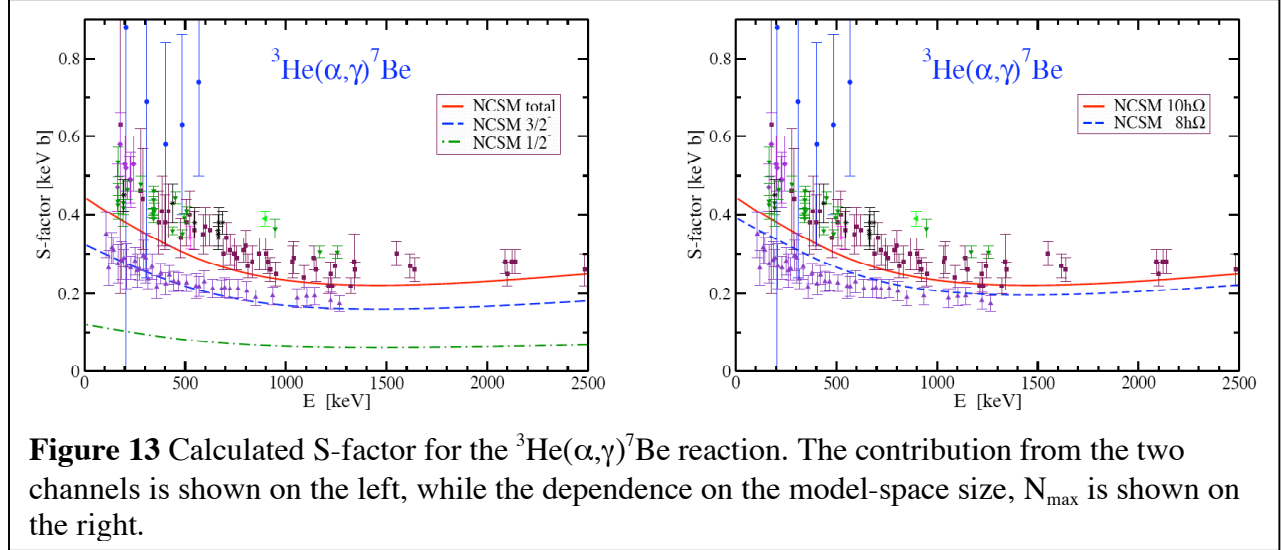


Figure 11 Calculated S-factor for the ${}^7\text{Be}(p,\gamma){}^8\text{B}$. In the left panel is the contribution from the $j=3/2$ and $j=1/2$ channels, while in the right panel the sensitivity to model space size is shown.

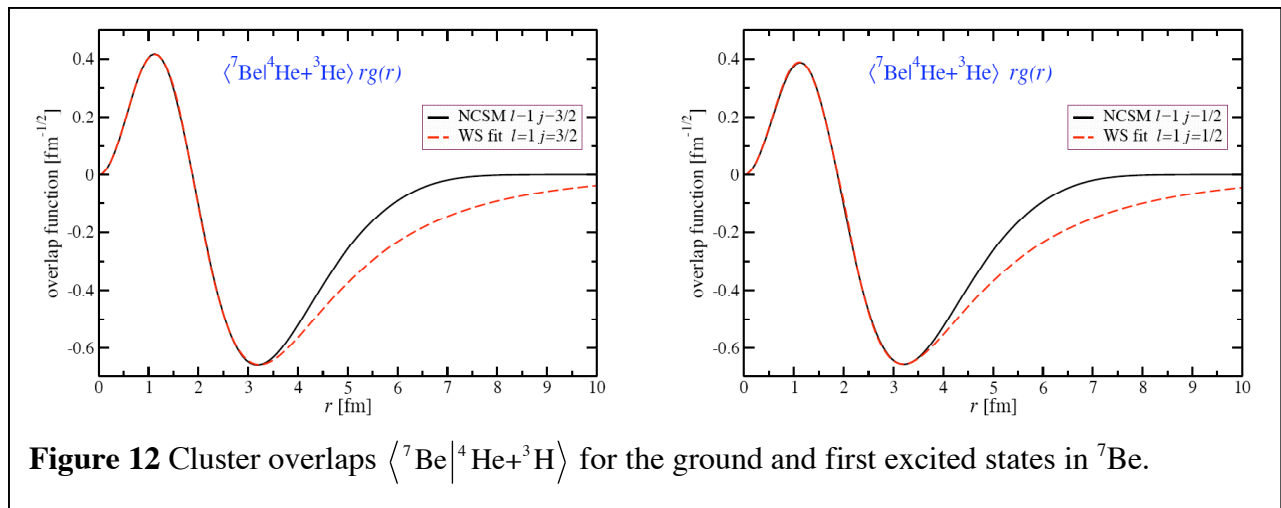
We note that the S-factor is very weakly dependent on the choice of the scattering-state potential at the low energies of interest. Our obtained S-factor is presented in Figure 11 where the contribution from the two partial waves is shown together with the total result (left panel). It is interesting to note a good agreement of our calculated S-factor with the recent Seattle direct measurement. The sensitivity of the S-factor to the size of the NCSM basis is also presented in Figure 11 (right panel). The overlap integrals were obtained in 6, 8 and $10\hbar\Omega$ calculations and independently corrected to insure the proper asymptotic behavior. The same scattering states were

used in all three cases. It is apparent that the sensitivity to the basis change is rather moderate. We observe a small oscillation at this frequency.

In order to judge the convergence of our S-factor calculation, we performed a detailed investigation of the model-space-size and the HO frequency dependencies. Based on this investigation we arrived at our theoretical S-factor value of $S_{17}(10 \text{ keV})=22.1\pm 1.0 \text{ eV b}$.



The ${}^3\text{He}(\alpha,\gamma){}^7\text{Be}$ capture reaction cross section was identified the most important uncertainty in the solar model predictions of the neutrino fluxes in the p-p chain. We investigated the bound states of ${}^7\text{Be}$, ${}^3\text{He}$ and ${}^4\text{He}$ within the *ab initio* NCSM and calculated the overlap functions of ${}^7\text{Be}$ bound states with the ground states of ${}^3\text{He}$ plus ${}^4\text{He}$ as a function of separation between the ${}^3\text{He}$ and the α particle. The obtained *p*-wave overlap functions of the ${}^7\text{Be}$ $3/2^-$ ground state and the ${}^7\text{Be}$ $1/2^-$ excited state are presented in the left and right panel, respectively, of Figure 12 by the full lines. The dashed lines show the corrected overlap functions obtained by the least-square fits of the WS parameters done in the same way as in the ${}^8\text{B}\leftrightarrow{}^7\text{Be}+p$ case. The corresponding NCSM spectroscopic factors obtained using the CD-Bonn 2000 in the $10\hbar\Omega$ model space for ${}^7\text{Be}$ and HO frequency of $\hbar\Omega=13 \text{ MeV}$ are 0.93 and 0.91 for the ground state and the first excited state of ${}^7\text{Be}$, respectively. We note



that contrary to the ${}^8\text{B} \leftrightarrow {}^7\text{Be} + p$ case, the ${}^7\text{Be} \leftrightarrow {}^3\text{He} + \alpha$ p -wave overlap functions have a node.

Using the corrected overlap functions and a ${}^3\text{He} + \alpha$ scattering state obtained using a potential model we calculated the ${}^3\text{He}(\alpha, \gamma){}^7\text{Be}$ S-factor. Our $10\hbar\Omega$ result is presented in the left panel of Figure 13. We show the total S-factor as well as the contributions from the capture to the ground state and the first excited state of ${}^7\text{Be}$. By investigating the model space dependence for $8\hbar\Omega$ and $10\hbar\Omega$ spaces (shown in the right panel of Figure 13, we estimate the ${}^3\text{He}(\alpha, \gamma){}^7\text{Be}$ S-factor at zero energy to be higher than 0.44 keV b, the value that we obtained in the discussed case shown in Figure 13.

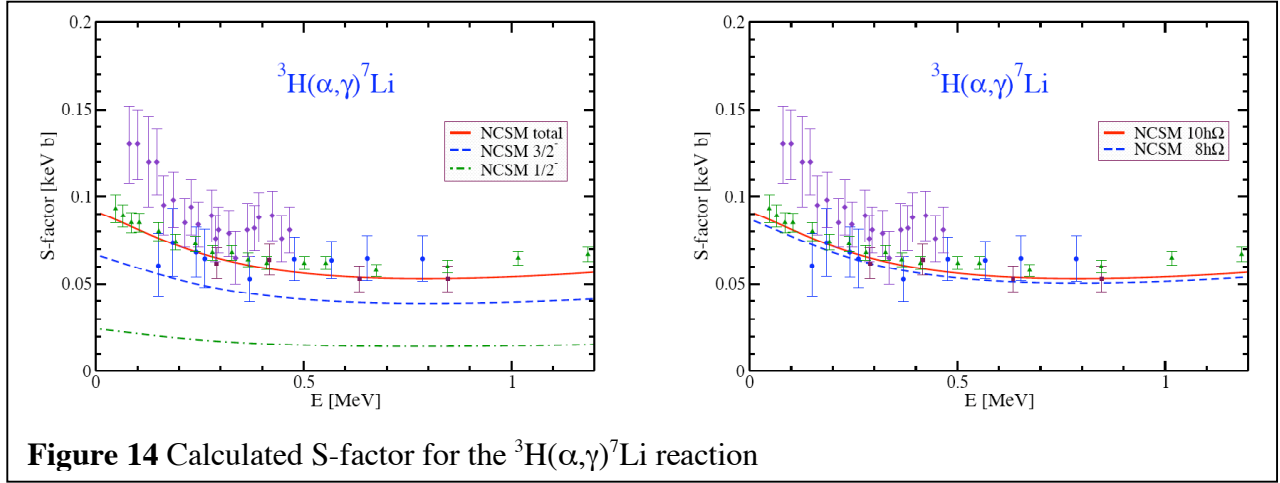


Figure 14 Calculated S-factor for the ${}^3\text{H}(\alpha, \gamma){}^7\text{Li}$ reaction

An important check on the consistency of the ${}^3\text{He}(\alpha, \gamma){}^7\text{Be}$ S-factor calculation is the investigation of the mirror reaction ${}^3\text{H}(\alpha, \gamma){}^7\text{Li}$, for which more accurate data exist. Our results obtained using the CD-Bonn 2000 NN potential are shown in Figure 14. It is apparent that our ${}^3\text{H}(\alpha, \gamma){}^7\text{Li}$ results are consistent with our ${}^3\text{He}(\alpha, \gamma){}^7\text{Be}$ calculation. We are on the lower side of the data and we find an increase of the S-factor as we increase the size of our basis. A positive fact is that this S-factor change is rather small, a sign of convergence of our calculation.

Our ${}^3\text{He}(\alpha, \gamma){}^7\text{Be}$ S-factor results were published together with the above ${}^7\text{Be}(p, \gamma){}^8\text{B}$

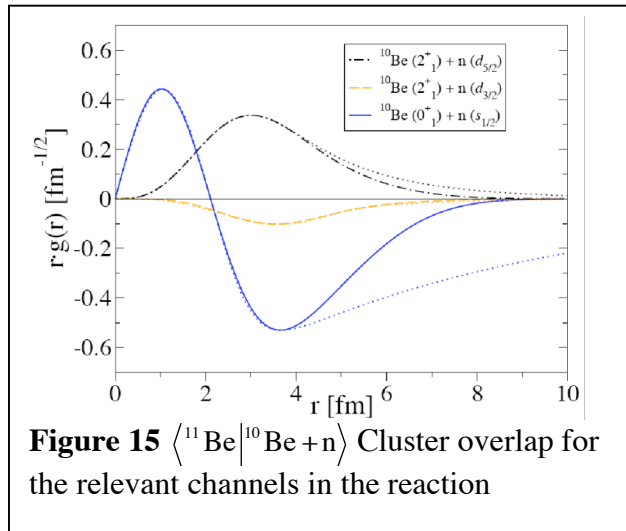


Figure 15 $\langle {}^{11}\text{Be} | {}^{10}\text{Be} + n \rangle$ Cluster overlap for the relevant channels in the reaction

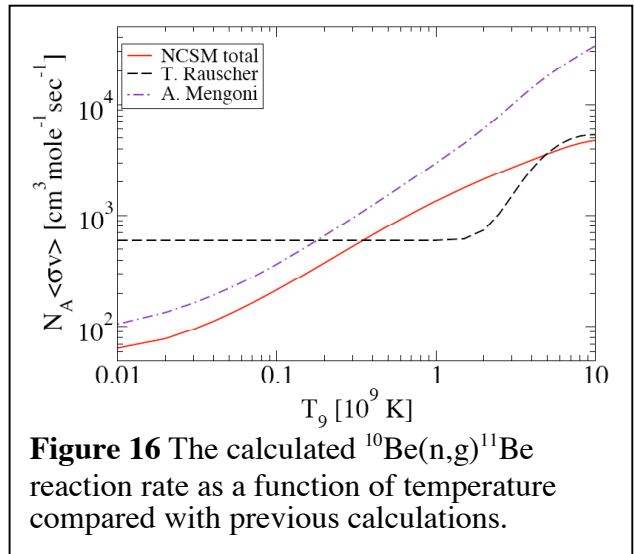


Figure 16 The calculated ${}^{10}\text{Be}(n, \gamma){}^{11}\text{Be}$ reaction rate as a function of temperature compared with previous calculations.

calculations as a refereed conference proceedings in Ref.²¹. Further, together with the ${}^3\text{H}(\alpha,\gamma){}^7\text{Li}$ S-factor results, these calculations will be published in Nuclear Physics A.

As a follow up to our detailed ${}^{11}\text{Be}$ investigation within the *ab initio* NCSM published in Ref.²², we performed calculation of the ${}^{10}\text{Be}(n,\gamma){}^{11}\text{Be}$ capture reaction rate. It has been suggested that inhomogenities in the distribution of baryons during the primordial nucleosynthesis can lead to the production of heavy elements. This occurs through a reaction network that consists predominantly of neutron capture reactions. One of the possible breakout chains is limited by the bottleneck reaction. We have studied this eaction using *ab initio* cluster overlaps of bound states fitted in the 0-4 fm range, see Figure 15. The nuclear eigenstates were obtained using the NCSM with the CD-Bonn 2000 interaction in model spaces up to $7\hbar\Omega$. The effective inter-fragment potentials that were obtained from the fit were also used to calculate the scattering states. The resulting reaction rate for this reaction is shown in Figure 16, compared to earlier estimates by T. Rauscher and A. Mengoni. Our calculations indicate that *p*-wave capture dominates at the relevant temperatures and that resonant capture is negligible. These results will most likely confirm the conclusion that ${}^8\text{Li}(a,n){}^{11}\text{B}$ is the relevant bottleneck in the inhomogeneous big bang reaction network; although a full simulation of the entire reaction network still has to be performed.

In the third year of the project, we made a breakthrough in the implementation of the RGM technique. We note that the RGM equations, the basis for our *ab initio* reaction theory, can be written schematically as

$$\sum_{\nu} \int d\vec{r} \left[\mathcal{H}_{\mu\nu}^{(A-a,a)}(\vec{r}', \vec{r}) - E \mathcal{N}_{\mu\nu}^{(A-a,a)}(\vec{r}', \vec{r}) \right] \Phi_{\nu}(\vec{r}) = 0$$

with \vec{r}, \vec{r}' the relative (Jacobi) coordinates of the distance between the centers of masses of the two interacting nuclei and the norm and Hamiltonian kernels defined by

$$\begin{aligned} \mathcal{N}_{\mu\nu}^{(A-a,a)}(\vec{r}', \vec{r}) &= \langle \Phi_{\mu\vec{r}'}^{(A-a,a)} | \hat{\mathcal{A}}^2 | \Phi_{\nu\vec{r}}^{(A-a,a)} \rangle \\ \mathcal{H}_{\mu\nu}^{(A-a,a)}(\vec{r}', \vec{r}) &= \langle \Phi_{\mu\vec{r}'}^{(A-a,a)} | \hat{\mathcal{A}} H \hat{\mathcal{A}} | \Phi_{\nu\vec{r}}^{(A-a,a)} \rangle \end{aligned}$$

The presence of the antisymmetrization operator $\hat{\mathcal{A}}$ makes these kernels nontrivial to compute. However, we discovered expressions that relate the Jacobi-coordinate matrix elements and the SD matrix elements needed to calculate the above kernels. These relations are of the type

$$\begin{aligned} \text{SD} \langle \Phi_{\mu n' \ell'}^{(A-1,1)JT} | P_{A,A-1} | \Phi_{\nu n \ell}^{(A-1,1)JT} \rangle \text{SD} &= \sum_{n_r, \ell_r, n'_r, \ell'_r, J_r} \langle \Phi_{\mu n'_r \ell'_r}^{(A-1,1)J_r T} | P_{(A-1,1)} | \Phi_{\nu n_r \ell_r}^{(A-1,1)J_r T} \rangle \\ &\times \sum_{NL} \hat{\ell} \hat{\ell}' \hat{J}_r^2 (-1)^{s+\ell_r-s'-\ell'_r} \begin{Bmatrix} s & \ell_r & J_r \\ L & J & \ell \end{Bmatrix} \begin{Bmatrix} s' & \ell'_r & J_r \\ L & J & \ell' \end{Bmatrix} \\ &\times \langle n_r, \ell_r, N L | 00 n \ell \rangle_{\frac{1}{A-1}} \langle n'_r, \ell'_r, N L \ell' | 00 n' \ell' \ell' \rangle_{\frac{1}{A-1}} \end{aligned}$$

Here, as an example, we explicitly show the transposition operator matrix element needed in the norm kernel. An analogous relation is valid for the Hamiltonian matrix elements needed in the Hamiltonian kernel. It is now possible to obtain the RGM kernels from second-quantization operator matrix elements calculated with the NCSM wave functions expanded in the SD basis. For example, for the above transposition operator we get

$$\begin{aligned}
SD \langle \Phi_{\mu n' \ell'}^{(A-1,1)JT} | P_{A,A-1} | \Phi_{\nu n \ell}^{(A-1,1)JT} \rangle_{SD} &= \frac{1}{A-1} \sum_{jj'K\tau} \left\{ \begin{matrix} I_1 \frac{1}{2} s \\ \ell J j \end{matrix} \right\} \left\{ \begin{matrix} I_1 \frac{1}{2} s' \\ \ell' J j' \end{matrix} \right\} \left\{ \begin{matrix} I_1 K I_1' \\ j' J j \end{matrix} \right\} \left\{ \begin{matrix} T_1 \tau T_1' \\ \frac{1}{2} T \frac{1}{2} \end{matrix} \right\} \\
&\times \hat{s} \hat{s}' \hat{j} \hat{j}' \hat{K} \hat{\tau} (-1)^{I_1 + j' + J} (-1)^{T_1 + \frac{1}{2} + T} \\
&\times SD \langle A - 1 \alpha' I_1' T_1' | | (a_{n\ell, j \frac{1}{2}}^\dagger \tilde{a}_{n'\ell', j' \frac{1}{2}})^{(K\tau)} | | A - 1 \alpha I_1 T_1 \rangle_{SD}
\end{aligned}$$

The Jacobi-coordinate matrix element is then obtained after combining the above relations by matrix inversion. We coded the above relations. The validity and correctness of both the relations and the code was later checked by our new postdoc, Sofia Quaglioni. She derived the Jacobi coordinate matrix element directly for the case of a single-nucleon projectile and checked that both approaches lead to the same result. Our ability to compute the RGM kernels using both types of coordinates allows us to investigate reactions between both the lightest nuclei where the Jacobi coordinate formulations is the most efficient and the heavier nuclei where the use of the Slater determinant basis is superior.

We are now continuing to develop the RGM technique and its coupling with the *ab initio* NCSM. We expect to perform the first scattering calculations using this fully *ab initio* formalism later this year. Augmenting the NCSM with the RGM to include clustering and resonant and non-resonant continuum offers our best hope to achieve an accurate description of nuclear reactions and alpha-clustering in e.g. ^{12}C and ^{16}O nuclei, which is one of the grand challenges in nuclear physics, as it dominates the production of carbon and oxygen, the critical elements of life, in the universe.

5 Electron Screening in a Thermal Plasma

Though the plasma screening and nuclear physics at high intensity laser facilities part of this project was unfortunately de-scoped because of budget constraints, we still did make some progress that is having an impact on future laser experimentation at the National Ignition Facility (NIF).

In the area of plasma screening of nuclear reactions, the weakly coupled, equilibrium theory due to Brown and Sawyer was verified and used as the motivator for a new, non-equilibrium expression for plasma screening to be used in multi-temperature plasmas such those that will be encountered in the ignition program at NIF. This expression was put in our main design codes and initial sensitivity studies were done on the impact of plasma screening on both the main D-T fusion reaction, and certain diagnostic fusion reaction pathways involving heavier elements.

We have also proposed a wide class of nuclear physics experiments applying laser fusion targets that show considerable promise as both fusion diagnostics and a window on multiple step, excited state nuclear reactions that would occur inside fusion capsules.

Many of these ideas were presented in invited and contributed talks at a variety of nuclear physics, high energy density physics, and plasma astrophysics meetings.

6 Benefits to LLNL

During the course of this LDRD, the Nuclear Theory and Modeling (NTM) Group has developed new theoretical methods and computational tools to perform *ab initio* studies of nuclear properties. This capability has grown considerably during the past seven years at LLNL, and largely due to LDRD investment. This investment has led to the NTM group emerging as an international leader in nuclear theory and has delivered a unique capability to LLNL to perform a serious *ab initio* studies of light-ion fusion reactions and that will help to reduce uncertainties present in data bases for nuclear reaction cross sections. Our enhanced leadership role is evidenced by several

events. The PI is assuming several community leadership positions regarding the proposed rare-isotope accelerator. The PI also presented a plenary talk at the Fall 2006 meeting of the Division Nuclear Physics to present the outlook for research in low-energy physics. Further, the PI was an organizer for the Nuclear Theory Working Group at the Study of Nuclei/Nuclear Astrophysics Town Meeting for the 2007 Long-range Plan. Steve Libby was a member of the Rare Isotope Science Assessment Committee convened by the National Academy of Sciences to assess the science case for the Rare Isotope Facility. Increasingly, our research team, especially Petr Navratil, is being invited to present the results of our research at several international conferences and summer schools. The highly successful work performed under this LDRD has significantly enhanced the research profile of LLNL in nuclear theory. From FY04-06, our DOE/SC/NP funding was \$75K, while in FY07 it increased to \$125K. Our research budget plan with the DOE/SC/NP indicates that this funding could grow to \$275 in FY08, and to nearly \$400K in FY09. Our success in research and utilizing the high-performance computing resources at LLNL has also enabled us to become the leading participant in the recent SciDAC-2 project: UNEDF: Universal Nuclear Energy Density Functional, where the NTM group is now receiving \$420K.

7 Publications

7.1 Refereed Journal Publications

1. Barrett, BR; Stetcu, I; Navratil, P; Vary, JP; From non-Hermitian effective operators to large-scale no-core shell model calculations for light nuclei, J. Phys. A-Math. Gen. 39, 9983 (2006).
2. A. Negret *et al.*, Gamow-Teller strengths in the A=14 multiplet: A challenge to the shell model, Phys. Rev. Lett. 97, 062502 (2006).
3. P. Navratil, C. A. Bertulani and E. Caurier, ${}^7\text{Be}(p,\gamma){}^8\text{B}$ S-factor from *ab initio* no-core shell model wave functions, Phys. Rev. C 73, 065801 (2006).
4. A. Nogga, P. Navratil, B. R. Barrett and J. P. Vary, Spectra and binding energy predictions of chiral interactions for ${}^7\text{Li}$, Phys. Rev. C 73, 064002 (2006).
5. P. Navratil, C. A. Bertulani and E. Caurier, ${}^7\text{Be}(p,\gamma){}^8\text{B}$ S-factor from *ab initio* wave functions, Phys. Lett. B. 634, 191 (2006).
6. E. Caurier and P. Navratil, Proton radii of ${}^{4,6,8}\text{He}$ isotopes from high-precision nucleon-nucleon interactions, nucl-th/0512015, Phys. Rev. C 73, 021302(R) (2006).
7. I. Stetcu, B. R. Barrett, P. Navratil and J. P. Vary, Long- and short-range correlations in the *ab initio* no-core shell model, Phys. Rev. C 73, 037307 (2006).
8. C. Forssen, P. Navratil, W. E. Ormand and E. Caurier, Large basis *ab initio* shell model investigation of ${}^9\text{Be}$ and ${}^{11}\text{Be}$. Phys. Rev. C 71, 044312 (2005).
9. I. Stetcu, B. R. Barrett, P. Navratil and J. P. Vary, Effective operators within the *ab initio* no-core shell model. Phys. Rev. C 71, 044325 (2005).
10. P. Navratil, *Ab initio* nuclear structure and nuclear reactions in light nuclei. Int. J. Mod. Phys. E 14, 85 (2005).
11. P. Navratil, C. Forssen, W. E. Ormand and E. Caurier, *Ab Initio* No-Core Shell Model Calculations Using Realistic Two- and Three-Body Interactions. Eur. Phys. J. A 25, 481-484 (2005).
12. P. Navratil, Cluster form factor calculation in the *ab initio* no-core shell model. Phys. Rev. C 70, 054324 (2004).
13. P. Navratil, Translationally invariant density. Phys. Rev. C 70, 014317 (2004).

14. T. C. Luu, S. Bogner, W. C. Haxton and P. Navratil, Effective interactions for the three-body problem. *Phys. Rev. C* **70**, 014316 (2004).
15. M. A. Hasan, J. P. Vary and P. Navratil, Hartree-Fock approximation for the *ab initio* no-core shell model. *Phys. Rev. C* **69**, 034332 (2004).
16. P. Navratil and E. Caurier, Nuclear structure with accurate chiral perturbation theory nucleon-nucleon potential: Application to ${}^6\text{Li}$ and ${}^{10}\text{B}$. *Phys. Rev. C* **69**, 014311 (2004).
17. H. Zhan, A. Nogga, B. R. Barrett, J. P. Vary and P. Navratil, Extrapolation method for the no-core shell model calculation. *Phys. Rev. C* **69**, 034302 (2004).

7.2 *Referred Conference Proceedings*

1. B R Barrett, P Navratil, A Nogga, W E Ormand, S Quaglioni, I Stetcu and J P Vary, New developments within the no-core shell model, *J. Phys.: Conf. Ser.* **49**, 1 (2006).
2. P. Navratil, C. A. Bertulani and E. Caurier, ${}^7\text{Be}(p,\gamma){}^8\text{B}$ S-factor from *ab initio* no-core shell model wave functions, *J. Phys.: Conf. Ser.* **49**, 15 (2006).
3. P. Navratil, *Ab initio* nuclear structure and nuclear reactions in light nuclei. *Int. J. Mod. Phys. E* **14**, 85 (2005).
4. Stetcu, I; Barrett, BR; Navratil, P; Johnson, CW; Electromagnetic transitions with effective operators. *Int. J. Mod. Phys. E* **14**, 95-103 (2005).
5. P. Navratil, C. Forssen, W. E. Ormand and E. Caurier, *Ab Initio* No-Core Shell Model Calculations Using Realistic Two- and Three-Body Interactions. *Eur. Phys. J. A* **25**, 481-484 (2005).
6. I. Stetcu, B. R. Barrett, P. Navratil, J. P. Vary, Effective Operators in the NCSM Formalism, *Eur. Phys. J. A* **25**, 489 (2005).
7. Nuclear physics with statistics, W.E. Ormand, *Int. J. Mod. Phys. E* **14**, 67 (2005).
8. P. Navratil, W. E. Ormand, E. Caurier and C. Bertulani, No-Core Shell Model and Reactions. 2nd Argonne/MSU/JINA/INT RIA Workshop on Reaction Mechanisms for Rare Isotope Beams. East Lansing, Michigan, March 9-12, 2005. Edited by B. A. Brown. *AIP Conference Proceedings* **791**, p. 32.
9. A. Nogga, E. Epelbaum, P. Navratil, W. Glockle, H. Kamada, Ulf-G Meissner, H. Witala, B. R. Barrett and J. P. Vary, Probing chiral interactions in light nuclei. *Nucl. Phys. A* **737**, 236 (2004).
10. Barrett, BR; Navratil, P; Nogga, A; Ormand, WE; Vary, JP; No-Core Shell-Model calculations in light nuclei with three-nucleon forces, *Nucl. Phys. A* **746**, 579C-582C (2004).
11. Vary, JP; Barrett, BR; Lloyd, R; Navratil, P; Nogga, A; Ormand, WE; Shell model in a first principles approach. *Nucl. Phys. A* **746**, 123C-129C (2004).
12. S. B. Libby, M. Tabak, R. D. Hoffman, M. A. Stoyer, S. W. Haan, S. P. Hatchett, D. P. McNabb, W. E. Ormand, J. Escher, P. Navratil, D. Gogny, M. S. Weiss, M. Mustafa, J. Becker, R. A. Ward, "Prospects for Investigating Unusual Nuclear Reaction Environments Using the National Ignition Facility," *Proceedings of the Third International Conference on Fusion Sciences and Applications*, Monterey, CA American Nuclear Society, (ANS Proceedings # 700313, pp 935-939, 2004).

7.3 *Invited Talks and Seminars*

1. P. Navratil, "Light nuclei from fundamental interactions", NPI Rez, Czech Republic, November 2006.
2. P. Navratil, "Helium radii & proton analysing powers in the NCSM", ECT* Trento,

- November 2006.
3. P. Navratil, "Light nuclei from fundamental interactions", N-Division Seminar, September 2006
 4. P. Navratil, "Applications of the Ab Initio No-Core Shell Model for Nuclear Structure and Reactions", P. Navratil, Nuclear Structure 06 (NS06), Oak Ridge, Tennessee, July 2006.
 5. P. Navratil, "Light nuclei from fundamental interactions", TU Darmstadt, Germany, July 2006.
 6. P. Navratil, " ${}^7\text{Be}(p,\gamma){}^8\text{B}$ S-factor from ab initio wave functions", GSI Darmstadt, Germany, July 2006
 7. P. Navratil, " ${}^7\text{Be}(p,\gamma){}^8\text{B}$ S-factor from ab initio wave functions", International Symposium on Structure of Exotic Nuclei and Nuclear Forces (SENUF 06) University of Tokyo, Japan, March 2006.
 8. P. Navratil, "Nuclear structure from chiral-perturbation-theory two- plus three-nucleon interactions", INT, University of Washington, Seattle, October 2005.
 9. P. Navratil, "Capture reactions important for astrophysics from ab initio wave functions", Nuclear Physics Institute, ASCR, Rez near Prague, Czech Republic, July 2005.
 10. P. Navratil, "Testing Nuclear Forces in Many-Body Calculations", Nuclear Forces and QCD: Never the Twain Shall Meet? ECT* Trento, Italy, June 2005.
 11. P. Navratil, "A Fundamental Theory of Light Ion Reactions", LLNL, PAT DRC talk, May 2005.
 12. P. Navratil, "No-Core Shell Model and Reactions", Second Argonne/MSU/JINA/INT RIA Workshop on Reaction Mechanisms for Rare Isotope Beams, March 2005.
 13. P. Navratil, "Ab Initio Nuclear Structure & Reactions", LLNL, N-Division TRC talk, February 2005.
 14. P. Navratil, "Nuclear structure from first principles: Ab initio no-core shell model", Argonne National Laboratory, November 2004.
 15. P. Navratil, "Effective Interactions from Similarity Transform in the No-Core Shell Model", Seattle, WA, Institute for Nuclear Theory, Nuclear Forces and the Quantum Many-Body Problem, October 2004.
 16. P. Navratil, "Nuclear structure from first principles: Ab initio no-core shell model for light nuclei.", Tokyo, Center for Nuclear Studies, 3rd CNS International Summer School, August 2004.
 17. P. Navratil, "Ab initio calculations for light nuclei using realistic two- and three-body interactions", APS April Meeting, Denver, CO, May 2004.
 18. P. Navratil, "Ab initio nuclear structure and nuclear reactions on light nuclei", Istanbul, Blueprints for the Nucleus: From First Principles to Collective Motion, May 2004.
 19. P. Navratil, "Direct reactions on light nuclei with nuclear structure from first principles", Workshop on Perspectives of polarization in RI-beam induced reactions, University of Tokyo, March 2004.
 20. P. Navratil, "Structure of light nuclei from first principles", Iowa State, March 2004.
 21. W.E. Ormand, "Towards a Deeper Understanding of the Nucleus with Exotic Nuclei", Plenary talk for the 2006 Fall Meeting of the Division of Nuclear Physics, Bull. Am. Phys. Soc. **51**, 16 (2006)
 22. W.E. Ormand, "The future of the shell model and radioactive-ion beam facilities", NSCL User Workshop, June 2006, East Lansing, MI, UCRL-PRES-221822
 23. W.E. Ormand, "Rare Isotope Science: Nuclear Theory", W.E. Ormand, Meeting of the Rare

- Isotope Science Assessment Committee, Feb. 2006, Irvine, CA, UCRL-PRES-218827
24. W.E. Ormand, "Nuclear Physics from Scratch", Invited talk at the 21st Winter Workshop on Nuclear Dynamics, Breckenridge, CO, 5-12 February 2005. UCRL-PROC-211856
 25. W.E. Ormand, "The No-Core Shell Model", Nuclear Forces and the Quantum Many-body Problem, Oct. 2004, Seattle
 26. W.E. Ormand, "The No-Core Shell Model", New Perspectives on P-shell Nuclei and Beyond, July, 2004, East Lansing
 27. W.E. Ormand, "Nuclear Physics with Statistics", Blueprints for the Nucleus: From First Principles to Collective Motion, May 17-23, 2004, Istanbul
 28. W.E. Ormand, "Surrogate Nuclear Reactions: Trying to do the Impossible", Nuclear Reactions on Unstable Nuclei and the Surrogate Reaction Technique, Jan 12-15, 2004, Asilomar, CA UCRL-PRES-201956
 29. W.E. Ormand, "Towards an Exact Description of the Structure of Light Nuclei", Annual Fall Meeting of the Division of Nuclear Physics, October 30 – November 1, 2003, Tucson, AZ
 30. S. B. Libby, "Prospects for Investigating Unusual Nuclear Reaction Environments Using the National Ignition Facility," The Third International Conference on Inertial Fusion Sciences and Applications, Monterey, California, September 9, 2003.
 31. S. B. Libby, "Prospects for Investigating Unusual Nuclear Reaction Environments Using the National Ignition Facility," SCIPP Seminar, University of California at Santa Cruz, Santa Cruz, CA, January 22, 2004;
 32. S. B. Libby, "Prospects for Investigating Unusual Nuclear Reaction Environments Using the National Ignition Facility," 5th International Conference on High Energy Density Laboratory Astrophysics, Tucson, Arizona, March 10-13, 2004.
 33. "Inertial Fusion Diagnostics and Prospects for Investigating Unusual Nuclear Reaction Environments at the National Ignition Facility," Nuclear Physics Seminar, University of Tennessee Physics Department, Knoxville, Tennessee, November 6, 2006.

8 Conclusions

Over the three-year period covered by LDRD funding, this project made significant progress towards achieving the ultimate goal of understanding the properties of nuclei from the fundamental interactions between the constituent protons and neutrons in a nucleus. Prior to this LDRD, most success towards this goal was limited to describing the structure of nuclei. Here, we explicitly focused on developing an entirely new framework for describing the dynamical processes governing nuclear reactions. We applied our reaction formalism to a series of reactions important in astrophysics. Excellent agreement between theory and experiment was achieved for the ${}^7\text{Be}(p,\gamma){}^8\text{B}$ reaction, which gives confidence in our result at the very low astrophysical energies, where experiment is not feasible. In this LDRD, we performed an extensive study of the three-nucleon interaction within the framework of effective field theory. This work has led to unique capabilities for the Nuclear Theory and Modeling Group at LLNL that will enable it to update and reduce uncertainties in nuclear reaction data bases. The success of this LDRD has dramatically increased the nuclear theory research profile at LLNL, and has led to a substantial increase in funding from the DOE Office of Science through the Nuclear Theory in the Office of Nuclear Physics and from SciDAC.

References

-
- ¹ J. N. Bahcall and M.H. Pinsonneault, Phys. Rev. Lett. **92**, 121301 (2004)
- ² J. N. Bahcall and R. K. Ulrich, Rev. Mod. Phys. **60**, 297 (1988); J. N. Bahcall, M. H. Pinsonneault, S. Basu, Astrophys J. **555**, 990 (2001); and references therein.
- ³ P.J. Brussaard and P.W.M. Glaudemans, Shell-model Applications in Nuclear Spectroscopy, (North Holland, Amsterdam, 1977)
- ⁴ R.D. Lawson, Theory of the nuclear Shell Model, (Clarendon Press, Oxford, 1980)
- ⁵ E. Caurier, G. Martinez-Pinedo, F. Nowacki, A. Poves, and A.P. Zuker, Rev. Mod. Phys. **77**, 427 (2005)
- ⁶ C. Lanczos, J. Res. Natl. Bur. Stand. **45**, 252 (1950)
- ⁷ E. Caurier and F. Nowacki, Acta Phys. Pol. B **30**, 705 (1999).
- ⁸ P. Navrátil and B.R. Barrett, Phys. Rev. C **54**, 2986 (1996); **57**, 3119 (1998); P. Navrátil and B.R. Barrett, Phys. Rev. C **57**, 562 (1998); P. Navrátil and B.R. Barrett, Phys. Rev. C **59**, 1906 (1999); P. Navrátil, G.P. Kamuntavicius, and B.R. Barrett, *ibid.* **61**, 044001 (2000).
- ⁹ K. Suzuki and S.Y. Lee, Prog. Theor. Phys. **64**, 2091 (1980); K. Suzuki, *ibid.* **68**, 246 (1982); K. Suzuki, Prog. Theor. Phys. **68**, 246 (1982); K. Suzuki and R. Okamoto, *ibid.* **70**, 439 (1983).
- ¹⁰ B. S. Pudliner *et al.*, Phys. Rev. C **56**, 1720 (1997); R. B. Wiringa, Nucl. Phys. **A631**, 70c (1998); R. B. Wiringa *et al.*, Phys. Rev. C **62**, 014001 (2000); S. C. Pieper *et al.*, Phys. Rev. C **64**, 014001 (2001).
- ¹¹ R. Machleidt, F. Sammarruca, and Y. Song, Phys. Rev. C **53**, R1483 (1996); R. Machleidt, Phys. Rev. C **63**, 024001 (2001).
- ¹² S.A. Coon and H.K. Han, Few-Body Syst. **30**, 131 (2001).
- ¹³ S. C. Pieper, V. R. Pandharipande, R. B. Wiringa, and J. Carlson, Phys. Rev. C **64**, 014001:1-21 (2001).
- ¹⁴ S. Weinberg, Phys. Lett. B **251**, 288 (1990); S. Weinberg, Nucl. Phys. B **363**, 3 (1991); C. Ordóñez and U. van Kolck, Phys. Lett. B **291**, 459 (1992); C. Ordóñez, L. Ray, and U. van Kolck, Phys. Rev. Lett. **72**, 1982 (1994); Phys. Rev. C **53**, 2086 (1996); U. van Kolck, Phys. Rev. C **49**, 2932 (1994).
- ¹⁵ D.R. Entem and R. Machleidt, Phys. Rev. C **68**, 041001 (2003).
- ¹⁶ P. Navratil, V.G. Gueorguiev, J.P. Vary, and W.E. Ormand, nucl-th/0701038, UCRL-JRNL-227256
- ¹⁷ P. Navratil, Cluster form factor calculation in the *ab initio* no-core shell model. Phys. Rev. C **70**, 054324 (2004).
- ¹⁸ P. Navratil, Translationally invariant density. Phys. Rev. C **70**, 014317 (2004).
- ¹⁹ P. Navratil, C. A. Bertulani and E. Caurier, ${}^7\text{Be}(p,\gamma){}^8\text{B}$ S-factor from *ab initio* wave functions, Phys. Lett. B. **634**, 191 (2006).
- ²⁰ P. Navratil, C. A. Bertulani and E. Caurier, ${}^7\text{Be}(p,\gamma){}^8\text{B}$ S-factor from *ab initio* no-core shell model wave functions, Phys. Rev. C **73**, 065801 (2006).
- ²¹ P. Navratil, C. A. Bertulani and E. Caurier, ${}^7\text{Be}(p,\gamma){}^8\text{B}$ S-factor from *ab initio* no-core shell model wave functions, J. Phys.: Conf. Ser. **49**, 15 (2006).
- ²² C. Forssen, P. Navratil, W. E. Ormand and E. Caurier, Large basis *ab initio* shell model investigation of ${}^9\text{Be}$ and ${}^{11}\text{Be}$. Phys. Rev. C **71**, 044312 (2005).